Pontifícia Universidade Católica
do Rio de Janeiro

Erick Freitas de Almeida

Robust Power Allocation and Precoding for Cell-Free and Multi-Cell Massive MIMO Systems

Dissertação de Mestrado

Dissertation presented to the Programa de Pós–graduação em Engenharia Elétrica of PUC-Rio in partial fulfillment of the requirements for the degree of Mestre em Engenharia Elétrica.

Advisor: Prof. Rodrigo Caiado de Lamare

Rio de Janeiro
September 2022

Pontifícia Universidade Católica
do Rio de Janeiro

Erick Freitas de Almeida

Robust Power Allocation and Precoding for Cell-Free and Multi-Cell Massive MIMO Systems

Dissertation presented to the Programa de Pós–graduação em Engenharia Elétrica of PUC-Rio in partial fulfillment of the requirements for the degree of Mestre em Engenharia Elétrica. Approved by the Examination Committee.

Prof. Rodrigo Caiado de Lamare
Advisor
CETUC – PUC-Rio

Prof. Lukas Tobias Nepomuk Landau
CETUC – PUC-Rio

Prof. Roberto Brauer Di Renna
CETUC – PUC-Rio

Dr. André Robert Flores Manrique
CETUC – PUC-Rio

Rio de Janeiro, September the 9th, 2022

Erick Freitas de Almeida

Mobile network specialist with seven years of experience in telecommunication industry at Architecture & Innovation Technology department. He received his Master of Business Administration (MBA) in Computer Engineering degree, from the Universidade Federal do Rio de Janeiro (UFRJ), in 2019, and Bachelor of Science in Electrical Engineering degree from the Universidade Veiga de Almeida (UVA), in 2017.

Bibliographic data

Freitas de Almeida, Erick

Robust Power Allocation and Precoding for Cell-Free and Multi-Cell Massive MIMO Systems / Erick Freitas de Almeida; advisor: Rodrigo Caiado de Lamare. – Rio de Janeiro: PUC-Rio, Departamento de Engenharia Elétrica, 2022.

v., 81 f: il. color. ; 30 cm

Dissertação (mestrado) - Pontifícia Universidade Católica do Rio de Janeiro, Departamento de Engenharia Elétrica.

Inclui bibliografia

1. Engenharia Elétrica – Teses. 2. Sistemas de Múltiplas Antenas Livres de Células;. 3. MIMO massivo;. 4. Alocação de Potência;. 5. Pré-codificadores em Downlink;. 6. Sistemas de Múltiplas Antenas em Múltiplas Células.. I. Caiado de Lamare, Rodrigo. II. Pontifícia Universidade Católica do Rio de Janeiro. Departamento de Engenharia Elétrica. III. Título.

CDD: 621.3

To my family, Camille, Cinara, Gabriel and Ricardo. To my beloved grandparents Ignês, Chico, Emília and Antônio. To my sincere friends.

Acknowledgments

First of all, I would like to express my eternal gratitude and respect to my advisor, Prof. Rodrigo C. de Lamare, for giving me great opportunity to pursue this Msc degree. Thanks to him, I was accepted in this master program and could realize this dream. This work wouldn't be possible without all his guidance, patience and collaboration. In all these years, I was able to learn countless subjects that made me a much better professional.

Second, I would like to thanks CETUC and Pontifical Catholic University of Rio de Janeiro (PUC-Rio)'s professors, staff and students. Without the collaborative environment, lessons, support and dedication, this project wouldn't be possible.

I'm honored to thanks TIM Brasil for encouraging this work, specially my directors Silmar Palmeira and Atila Xavier, my manager Bruno Miranda, plus my colleagues in the CTIO. They have created excellent professional environment and have always been inspirations for me. Their tremendous support since the beginning of this chapter of my life was essential.

I would like to express all my endless gratitude and love to my family, Camille, Cinara, Gabriel and Ricardo. Their emotional support during all my MSc degree has been a corner stone to my success. I couldn´t have completed this task without their endless faith in me and my capacities.

I would like to thank the other members of my defence committee, Prof. Lukas Tobias Nepomuk Landau, Prof. Roberto Brauer Di Renna and Dr. André Robert Flores Manrique, for your time, patience and for giving me the honour to present my work.

I wish to thank CAPES and PUC-Rio for the financial support. This study was financed in part by the Coordenação de Aperfeiçoamento de Pessoal de Nível Superior - Brasil (CAPES) - Finance Code 001.

Finally, to all the people and institutions mentioned in this acknowledgement section, you made me a better person towards life. I hope my work is a source of pride for Emília and Ignês.

Abstract

Freitas de Almeida, Erick; Caiado de Lamare, Rodrigo (Advisor). **Robust Power Allocation and Precoding for Cell-Free and Multi-Cell Massive MIMO Systems**. Rio de Janeiro, 2022. 81p. Dissertação de mestrado – Departamento de Engenharia Elétrica, Pontifícia Universidade Católica do Rio de Janeiro.

Multi-Cell (MC) systems are present in mobile network operations from the first generation to the fifth generation of wireless networks, and considers the signals of all users to a base station (BS) centered in a cell. Cell-Free (CF) systems explore a large number of distributed antennas serving users at the same time. In this context, Multiple-input multiple-output (MIMO) techniques are used in both topologies and result in performance gains and interference reduction. In order to achieve the benefits mentioned, proper precoder design and power allocation techniques are required in the downlink (DL). In general, DL schemes assume perfect channel state information at the transmitter (CSIT), which is not realistic. This master thesis studies MC and CF with MIMO systems equipped with linear precoders in the DL and proposes an adaptive algorithm to allocate power in the presence of imperfect CSIT. The developed robust adaptive power allocation outperforms standard adaptive (APA) and uniform power allocation (UPA). Simulations also compare the performance of both systems frameworks using MMSE precoders with robust adaptive power allocation and adaptive power allocation.

Keywords

Cell-Free Massive MIMO; Massive MIMO; Power Allocation; Downlink Precoding; Multi-Cell Massive MIMO.

Resumo

Freitas de Almeida, Erick; Caiado de Lamare, Rodrigo. **Pré-Codificação MMSE e Alocação de Potência Iterativa para Sistemas de Múltiplas Antenas e Livres de Células**. Rio de Janeiro, 2022. 81p. Dissertação de Mestrado – Departamento de Engenharia Elétrica, Pontifícia Universidade Católica do Rio de Janeiro.

Os sistemas de múltiplas células (MC) estão presentes em operações de redes móveis desde a primeira geração (1G) até a quinta geração de redes sem fio (5G) e consideram os sinais de todos os usuários para uma estação base (BS) centralizada em uma célula. Os sistemas livres de célula (CF) exploram um grande número de antenas distribuídas atendendo os usuários simultaneamente. Nesse contexto, técnicas de sistemas múltiplas entradas e múltiplas saídas (MIMO) são utilizadas em ambas as topologias e resultam em ganhos de desempenho e redução de interferências. A fim de alcançar os benefícios mencionados, o sistema requer um projeto de pré-codificador adequado e utilização técnicas de alocação de potência no *downlink* (DL). Em geral, os esquemas DL assumem informações do estado do canal perfeitas na transmissão (CSIT), o que não é realista. Este trabalho estuda MC e CF com sistemas MIMO equipados com pré-codificadores lineares no DL e propõe um algoritmo adaptativo para alocação de potência na presença de CSIT imperfeito. A alocação de potência adaptativa robusta desenvolvida supera a alocação de potência adaptativa (APA) e uniforme padrão (UPA). As simulações também comparam o desempenho de ambas as estruturas de sistemas usando pré-codificadores MMSE com alocação de energia adaptativa robusta e alocação de energia adaptativa.

Palavras-chave

Sistemas de Múltiplas Antenas Livres de Células; MIMO massivo; Alocação de Potência; Pré-codificadores em Downlink; Sistemas de Múltiplas Antenas em Múltiplas Células.

Table of contents

List of figures

List of tables

List of Algorithms

List of Abbreviations

1G – First Generation Mobile Communications System
2G – Second Generation Mobile Communications System
3G – Third Generation Mobile Communications System
4G – Fourth Generation Mobile Communications System
5G – Fifth Generation Mobile Communications System
6G – Sixth Generation Mobile Communications System
APA – Adaptive Power Allocation
AP – Access Point
APS – Access Point Selection
BS – Base Station
BER – Bit Error Rate
CAPES – *Coordenação de Aperfeiçoamento de Pessoal de Nível Superior*
CAS – Co-located Antenna Systems
CB – Conjugate Beamforming
CDI – Channel Direction Information
CETUC – Center for Telecommunications Studies
CoMP – Coordinated Multi-Point Joint Processing
CPU – Central Processing Unit
CSI – Channel State Information
DAS – Distributed Antenna Systems
EE – Energy Efficiency
LS – Large-Scale Fading
M2M – Machine-to-Machine
MF – Matched Filter
MIMO – Multiple-Input Multiple-Output
MMSE – Minimum Mean-Square Error
MSE – Mean-Square Error
OPA – Optimal Power Allocation
QPSK – Quadrature Phase Shift Keying
RRH – Remote Radio Head
RV – Random Variable
SE – Spectral Efficiency
SG – Stochastic Gradient

SINR – Signal-to-interference-plus-noise ratio
SNR – Signal-to-noise ratio
TDD – Time Division Duplex
UPA – Uniform Power Allocation
ZF – Zero-Forcing

List of Symbols

L - number of APs

N - number of antenna elements per AP

M - total number of antenna elements

K - number of users

$h_{m,k}$ - channel coefficient between the mth antenna element and the kth user, where $h_{m,k} \in \mathbb{C}^{1\times1}$

$\hat{h}_{m,k}$ - channel estimation coefficient between the mth antenna element and the kth user, where $\hat{h}_{m,k} \in \mathbb{C}^{1\times1}$

$\tilde{h}_{m,k}$ - channel estimation error coefficient between the mth antenna element and the kth user, where $\tilde{h}_{m,k} \in \mathbb{C}^{1\times1}$

$\mathbf{h}_k$ - channel vector for user k, where $\mathbf{h}_k \in \mathbb{C}^{M\times1}$

$\hat{\mathbf{h}}_k$ - channel estimation vector for user k, where $\hat{\mathbf{h}}_k \in \mathbb{C}^{M\times1}$

$\tilde{\mathbf{h}}_k$ - channel estimation error vector for user k, where $\tilde{\mathbf{h}}_k \in \mathbb{C}^{M\times1}$

$\hat{\mathbf{h}}_m$ - channel estimation vector for the mth antenna, where $\hat{\mathbf{h}}_m \in \mathbb{C}^{1\times K}$

$\mathbf{H}_{MC}$ - channel matrix, where $\mathbf{H} \in \mathbb{C}^{K\times M}$

$\mathbf{H}_{CF}$ - channel matrix, where $\mathbf{H} \in \mathbb{C}^{M\times K}$

$\hat{\mathbf{H}}$ - channel estimation matrix, where $\hat{\mathbf{H}} \in \mathbb{C}^{K\times M}$

$\tilde{\mathbf{H}}$ - channel estimation error matrix, where $\tilde{\mathbf{H}} \in \mathbb{C}^{K\times M}$

$\boldsymbol{\beta}$ - large-scale fading matrix, where $\boldsymbol{\beta} \in \mathbb{R}^{M\times K}$

$\beta_{m,k}$ - large-scale fading coefficient between the mth antenna element and the kth user, where $\beta_{m,k} \in \mathbb{R}^{1\times1}$

$\boldsymbol{\beta}_k$ - large-scale fading vector associated to the kth user, where $\boldsymbol{\beta}_k \in \mathbb{R}^{M\times1}$

$\alpha_{m,k}$ - variance of $h_{m,k}$, where $\alpha_{m,k} \in \mathbb{R}^{1\times1}$

$\mathrm{PL}_{m,k}$ - path loss coefficient between the mth antenna element and the kth user, where $\mathrm{PL}_{m,k} \in \mathbb{R}^{1\times1}$

σ_{sh} - shadow fading standard deviation

$z_{m,k}$ - shadowing coefficient, where $z_{m,k} \in \mathbb{R}^{1\times1}$

$d_{m,k}$ - distance between the mth antenna element and the kth user

f_{freq} - carrier frequency in MHz

h_{m} - BS antenna height in meters

h_{AP} - AP antenna height in meters

h_{u} - user antenna height in meters

τ - length of pilot sequences

$\mathbf{\Pi}_k$ - transmit pilot sequence by the kth user, where $\mathbf{\Pi}_k \in \mathbb{C}^{\tau \times 1}$

$\mathbf{y}_m$ - received signal sequence by the mth antenna in the training step, where $\mathbf{y}_m \in \mathbb{C}^{\tau \times 1}$

ρ_r - uplink power

$\mathbf{w}_m$ - is the additive noise received by the mth user, where $\mathbf{w}_m \in \mathbb{C}^{\tau \times 1}$

y_k - signal received by the kth user, where $y_k \in \mathbb{C}^{1 \times 1}$

$\mathbf{y}$ - vector combining the signal received by all users, where $\mathbf{y} \in \mathbb{C}^{K \times 1}$

ρ_f - maximum transmitted power of each antenna

$\mathbf{P}$ - generic precoding matrix, where $\mathbf{P} \in \mathbb{C}^{M \times K}$

$\mathbf{s}$ - zero mean symbol vector, where $\mathbf{s} \in \mathbb{C}^{K \times 1}$

s_k - data symbol intended for user k, where $s_k \in \mathbb{C}^{1 \times 1}$

σ_s^2 - symbol variance

$\mathbf{C}_s$ - symbol covariance matrix, $\mathbf{C}_s \in \mathbb{R}^{K \times K}$

w_k - additive noise for user k, where $w_k \in \mathbb{C}^{1 \times 1}$

$\mathbf{w}$ - additive noise vector, where $\mathbf{w} \in \mathbb{C}^{K \times 1}$

σ_w^2 - noise variance

SNR - signal-to-noise ratio

$\mathbf{C}_w$ - noise covariance matrix, $\mathbf{C}_w \in \mathbb{R}^{K \times K}$

B - bandwidth in Hz

$R_{\text{k,CB}}$ - achievable rate of user k with CB precoding

R_{CB} - sum-rate with CB precoding

$\text{SINR}_{\text{k,CB}}$ - SINR of user k with CB precoding

$\beta_m^{\max}$ - largest coefficient in vector $\boldsymbol{\beta}_m$, where $\beta_m^{\max} \in \mathbb{R}^{1 \times 1}$

$R_{\text{k,ZF}}$ - achievable rate of user k with ZF precoding

R_{ZF} - sum-rate with ZF precoding

$\text{SINR}_{\text{k,ZF}}$ - SINR of user k with ZF precoding

$\boldsymbol{\psi}$ - auxiliary vector related to the desired signal of all users, where $\boldsymbol{\psi} \in \mathbb{C}^{K \times 1}$

ψ_k - the kth element of vector $\boldsymbol{\psi}$, where $\psi_k \in \mathbb{C}^{1 \times 1}$

$\boldsymbol{\phi}_k$ - auxiliary vector related to the interference in user k created by all other users, where $\boldsymbol{\phi}_k \in \mathbb{C}^{(K-1) \times 1}$

$\phi_{k,i}$ is the ith element of vector $\boldsymbol{\phi}_k$, where $\phi_{k,i} \in \mathbb{C}^{1 \times 1}$

$\boldsymbol{\gamma}_k$ - auxiliary vector related to the CSI error, where $\boldsymbol{\gamma}_k \in \mathbb{C}^{K \times 1}$

$\gamma_{k,i}$ - the ith element of vector $\boldsymbol{\gamma}_k$, where $\gamma_{k,i} \in \mathbb{C}^{1 \times 1}$

$\boldsymbol{\delta}_m$ - auxiliary vector related to the precoder energy, where $\boldsymbol{\delta}_m \in \mathbb{C}^{K \times 1}$

$\delta_{m,i}$ - the ith element of vector $\boldsymbol{\delta}_m$, where $\delta_{m,i} \in \mathbb{C}^{1 \times 1}$

SINR_k - signal-to-interference-plus-noise ratio of user k

$\mathbf{N}$ - power allocation matrix, where $\mathbf{N} \in \mathbb{R}_+^{K \times K}$

$\eta_{m,k}$ - power coefficient used by the mth antenna for transmission to user k, where $\eta_{m,k} \in \mathbb{R}_+^{1 \times 1}$

$\eta''_{m,k}$ - power coefficient used by the mth antenna for transmission to user k, where $\eta''_{m,k} = \sqrt{\eta_{m,k}}$

η_m - power coefficient of the mth antenna, where $\eta_m \in \mathbb{R}_+^{1\times 1}$

η_k - power coefficient of user k, where $\eta_k \in \mathbb{R}_+^{1\times 1}$

$\boldsymbol{\eta}$ - power coefficient vector, where $\boldsymbol{\eta} \in \mathbb{R}_+^{K\times 1}$

f - initial normalization factor of the MMSE precoder, where $f \in \mathbb{R}_+^{1\times 1}$

$\mathbf{x}$ - transmitted signal, where $\mathbf{x} \in \mathbb{C}^{M\times 1}$

x_m - transmitted signal by the mth antenna element, where $x_m \in \mathbb{C}^{1\times 1}$

E_{tr} - total transmitted power

λ - Lagrange multiplier

$\mathbf{A}$ - MMSE precoder combined with power allocation, where $\mathbf{A} \in \mathbb{C}^{M\times K}$

$\mathbf{a}_m$ - the mth row of matrix $\mathbf{A}$, where $\mathbf{a}_m \in \mathbb{C}^{1\times K}$

$\mathbf{P}_{\text{ZF}}$ - ZF precoder with power allocation, where $\mathbf{P}_{\text{ZF}} \in \mathbb{C}^{M\times K}$

$\mathbf{P}_{\text{MMSE}}$ - MMSE precoder with total power constraint, where $\mathbf{P}_{\text{MMSE}} \in \mathbb{C}^{M\times K}$

f_{MMSE} - final normalization factor of the MMSE precoder with total power constraint, where $f_{\text{MMSE}} \in \mathbb{R}_+^{1\times 1}$

$\mathbf{I}_D$ - identity matrix of size $D \times D$

$\mathbf{N}_{\text{MMSE}}$ - final power allocation matrix for the MMSE precoder with total power constraint, where $\mathbf{N}_{\text{MMSE}} \in \mathbb{R}_+^{K\times K}$

$R_{\text{k,MMSE}}$ - achievable rate of user k with MMSE precoding with total power constraint

R_{MMSE} - sum-rate with MMSE precoding with total power constraint

$\text{SINR}_{\text{k,MMSE}}$ - SINR of user k with MMSE precoding with total power constraint

T_{OPA} - number of iterations of the OPA algorithm

μ - step size of the APA algorithm

T_{APA} - number of iterations of the APA algorithm

$T_{\text{R-APA}}$ - number of iterations of the R-APA algorithm

$(\cdot)^*$ - complex conjugate

$(\cdot)^T$ - transpose

$(\cdot)^H$ - Hermitian operator

$\mathbb{E}[\cdot]$ - expected value

$\text{tr}(\cdot)$ - trace of a matrix

$\text{Re}(\cdot)$ - real part of the argument

$\|\cdot\|_2$ - Euclidean norm

$\|\cdot\|_F$ - Frobenius norm

$\odot$ - Hadamard or element-wise product

$\text{diag}\{\mathbf{D}\}$ - retains the main diagonal elements of a generic matrix $\mathbf{D}$ in a column vector

$x \sim \mathcal{N}(0, \sigma^2)$ - Gaussian random variable (RV) x with zero mean and variance σ^2

$x \sim \mathcal{CN}(0, \sigma^2)$ - circularly symmetric complex Gaussian RV x with zero mean and variance σ^2

1
Introduction

Broadband wireless cellular networks have passed through many generations over the last 30 years. The fifth generation (5G) is now being commercialized by the Mobile Network Operators (MNOs) since its cellular telecommunications standard specifications were defined by 3rd Generation Partnership Project (3GPP), national spectrum auctions were performed worldwide for licensing frequency bands, along with user's data consumption and data rate demand increases. In order to characterize 5G systems, we can cite higher data rates, lower latency, reduced energy consumption, interference management, massive connectivity, and ultra-reliability [1] as big advantages when compared to previous technologies.

Multiple-input multiple-output (MIMO) wireless technology was adopted in the third generation (3G) [2] and has been under extensive study ever since. MIMO techniques consist of multiple antennas employed at the transmitter and/or at the receiver. The main advantage of these systems is that they dramatically increase the overall throughput without the need for additional bandwidth [3]. By simultaneous transmission of multiple data streams which share the same time-frequency resources, we have numerous benefits of MIMO technology helping to achieve such significant performance gains: Array gain, spatial diversity gain, spatial multiplexing gain and interference reduction [4].

A tremendous number of connected user equipments (UEs) and high data rates are basic specifications for 5G systems and these demands tend to grow nowadays and are likely to increase even more in the following years. Massive MIMO techniques [5–7] were proposed and combined with several other enabling techniques to entitle 5G arrival and we can assume that it will be present in next generations. In terms of telecommunication architectural setup, multiple antennas are implemented to provide high beamforming and spatially multiplexing gain, thus achieving the high spectral efficiency (SE), energy efficiency, and link reliability to a massive number of users. As mentioned, the explosive demand for higher data rates and traffic volume is continuous, therefore wireless communication networks are required to provide better coverage, and uniform user performance over a wide coverage area [8].

In order to address the requirements of UEs in terms of performance

over a geographic area, we present two types of setups of antennas that can be discussed for the network deployment, aiming at different performances and benefits: co-located antenna system (CAS) and distributed antenna systems (DAS). In CAS design, the base station (BS) is often located at the center of each cell and low backhaul requirements are required. This setup has been applied since 1G and is considered for Multi-Cellular (MC) clusters architecture, which is spread out in global scale. This deployment is conventionally used for 5G systems and relies on frequency reuse, where users in geographically separated cells simultaneously use the same carrier frequency [9]. The cellular layout brings the possibility to increase the capacity of the system in a region, however, it faces challenges due to fading, path loss, and interference. Furthermore, each user is served by the BS responsible for the cell where the user is located, increasing inter-cell interference (ICI) and decreasing the performance at cell edge [10].

Most of the traffic congestion in cellular networks nowadays is at the cell edge, as a consequence of ICI and handovers. For that reason, traditional network design for 5G networks remains mediocre and suffer to satisfy 95% likely user data rates to 95% of the users [11]. Based on that, other techniques emerge to improve wireless communication and assist in the development of the sixth generation (6G), such as DAS design [12]. This setup can be used to minimize cell-edge interference, providing better coverage, since the base stations (BSs) are distributed in a wide area. In addition, cooperative multipoint joint processing (CoMP) is proposed to reduce inter-cell interference. Combining the advantages of massive MIMO, the CoMP and DAS techniques [13], the concept of Cell-Free (CF) systems has emerged, which is strongly considered for 6G networks.

Cell-Free Systems considers a large number of randomly located access points (APs) serving simultaneously a number of users over a wide area. This approach can reduce inter-cell interference through coherent cooperation between base stations. In this MIMO case, the APs cooperate via advanced backhaul links to jointly transmit signals in the downlink and jointly detect signals in the uplink [14].

1.1 Motivation

Wireless communication networks are under constant evolution and constitute a vast field of study. Considering all the previews and future network generations, MC systems are an established implementation currently used for 5G and CF systems are likely to be used for upcoming generations. Although

CF systems are quite recent, Zero Forcing (ZF) and Conjugated Beamforming (CB) precoding schemes with optimal power allocation (OPA) and uniform power allocation (UPA) were studied in [13], [15], [16]. Many works have considered minimum mean-square error (MMSE) precoders in MIMO systems, and the analysis with their implementation on CF are present in [16], [17].

Considering MIMO linear precoders design, perfect channel state information at the transmite side (CSIT) is required. In this work, we examine the application of adaptive power allocation (APA) techniques that aim to minimize the effect of interference [18]. Furthermore, robust adaptive power allocation (R-APA) for MC development in [19, 20] can help us to bring an effective approach for R-APA in CF systems.

Real-world systems do not meet the perfect CSIT assumption, and spectrum techniques that are used to obtain CSI introduce imperfections that can heavily degrade the systems. Consequently, the design of precoding and power allocation approaches, which consider imperfect CSIT, is of great significance. In addition, the shortage of studies in the literature involving MMSE precoders in CF system bring excellent opportunities to the theme.

1.2 Contributions

In this work, we study MC and CF along with massive MIMO systems equipped with linear MMSE precoders in the downlink (DL). We propose R-APA algorithms to allocate power in the presence of imperfect CSIT that outperforms APA and standard UPA. Simulation results illustrate the performance of the proposed R-APA algorithms used in conjunction with MMSE precoders against existing techniques in MC and CF scenarios.

1.3 Thesis Outline

This thesis is structured as follows. Chapter II review the literature involved in MIMO systems and describes MC and CF systems models. Chapter III presents the linear precoding scheme adopted, the proposed R-APA algorithms and discuss the numerical results, which compare MC and CF networks in terms of Sum Rates and Bit Error Rate (BER). Then, we draw some conclusions over both systems and mention some future works in Chapter IV.

1.4 Notation

See List of Symbols on pages 15-18.

1.5 List of Publications

Some results of this thesis are under review in the following conference paper submission:

– Erick F. de Almeida, Rodrigo C. de Lamare, "Seleção de Pontos de Acesso, Pré-Codificação MMSE e Alocação de Potência Iterativa para Sistemas de Múltiplas Antenas Livres de Células", *XL Simpósio Brasileiro de Telecomunicações e Processamento de Sinais (SBrT)*, 2022, submitted.

2
Multi-Cell and Cell-Free Massive MIMO Systems Review

In this chapter, we review the literature on massive MIMO, CAS, DAS and cooperative networks that have lead to the development of multi-cell and cell-free massive MIMO systems. We will also cover some channel properties, modulation fundamentals and propagation effects. Uplink and downlink communication links are studied in detail. Next, we will provide an overview on precoding and power allocation along with their benefits and applications. Finally, we will describe the multi-cell and cell-free system models.

2.1
Literature Review

In this section, we present a literature review of key concepts used throughout this thesis such as massive MIMO, modulation and propagation aspects, channel modeling and its capacity. We also review precoding and power allocation concepts that are widely used in massive MIMO systems. We then describe in detail uplink and downlink system models for multi-cell and cell-free networks using linear algebra.

2.1.1
Massive MIMO

In wireless communication networks, multiple users may communicate at the same time and/or frequency. The more aggressive the reuse of time and frequency resources, the higher the network capacity will be, provided that transmitted signals can be detected reliably. Multiple users may be separated in time (time-division), frequency (frequency-division), code (code-division), etc. [4]. Massive MIMO is a MIMO system, with a very large number of antennas at the transmission for DL, in order to multiplex messages to several users sharing the same time-frequency resource [21]. MIMO features have been used since 3G due to its benefits listed below:

– Array gain: increase in receive Signal-to-Noise Ratio (SNR) that results from a coherent combining effect of the wireless signals to a receiver;

– Spatial diversity gain: Mitigates fading and is realized by providing the receiver with multiple (ideally independent) copies of the transmitted signal in space, frequency or time;
– Spatial multiplexing gain: provides an extra dimension to separate users, allowing more aggressive reuse of time and frequency resources, thereby increasing the network capacity. In general, the number of data streams that can be reliably supported by a MIMO channel equals the minimum of the number of transmit antennas and the number of receive antennas;
– Interference reduction and avoidance: multiple users share the same time and frequency.

To characterize this wireless communication technique, N_r is considered the number of receive antennas (Rx) and N_t the number of transmit antennas (Tx). The direction of the connection can be described as matrix with dimensions $N_t \times N_r$ for the uplink (UL) and $N_r \times N_t$ for the DL. By employing multiple antennas at the Tx and/or the Rx, MIMO systems provide spatial multiplexing and/or diversity gains mentioned before.

To illustrate, suppose that a BS is equipped with N_t antennas and K independent users are equipped with N_u antennas as demonstrated in Fig. 2.1. This system can be considered as $(KN_u \times N_t)$ for a downlink or $(N_t \times KN_u)$ for the uplink. In this multi-user communication system, multiple antennas allow the independent users to transmit their own data stream in the uplink at the same time or the base station to transmit the multiple user data streams to be decoded by each user in the downlink. This is attributed to the increase in degrees of freedom with multiple antennas as in the single-user MIMO system [22].

In single-user MIMO (SU-MIMO), the dimensions of the system are limited by the number of antennas that can be accommodated on a mobile device. However, by having each BS communicating with several users concurrently, the multiuser version of MIMO (MU-MIMO) can effectively pull together the antennas at those users and overcome this bottleneck. In the downlink studied in detail in this work, the channel matrix has a different structure for SU-MIMO is given by $\mathbf{H} \in \mathbb{C}^{1\times N_t}$. Similarly, for the MU-MIMO system, we have $\mathbf{H} \in \mathbb{C}^{KN_u\times N_t}$.

In terms of network architecture, there is a certain amount of possible setups for massive MIMO. In this work, we can cite co-located antenna systems (CAS) and distributed antenna systems (DAS). In a CAS system, a base station (BS) is co-located at the center of each cell, with the advantage of low backhaul requirement. This architectural scheme has been under study

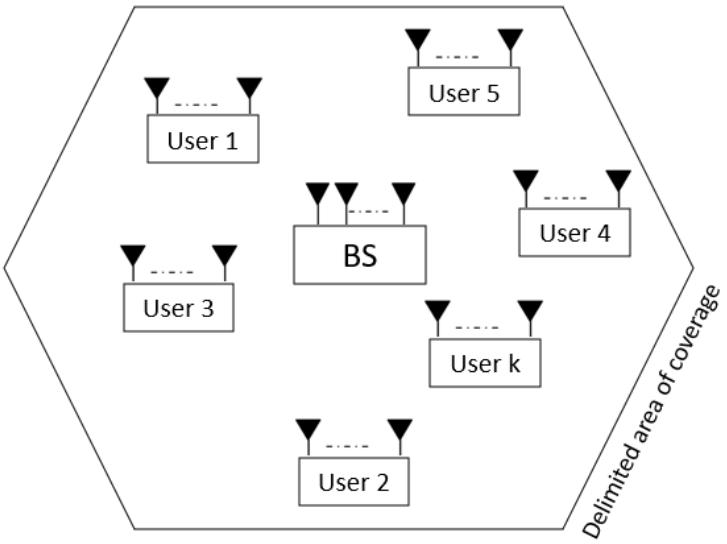

Figure 2.1: Regular Cellular System Multi-User MIMO Communication with K=6.

since 1G, having many works on the field in [23], and [13]. Furthermore, it will be considered for multi-cell systems in this work. Contrarily, in DAS systems, remote radio heads (RRHs) are spread all over the cell and connected to a central processor (CP) by optical fiber, coaxial cable or microwave [12].

Coordinated multi-point joint processing (CoMP) transmission/reception, promote multiple BSs cooperating and acting as a single effective MIMO transceiver, enabling the exploitation of interference, taking advantage of joint signal processing rather than treating it as noise, promising vast gains in spectral efficiency and fairness. As another direction on MIMO technology, CoMP and network MIMO have been proposed in [3], [24], [25], [26] aiming to improve SE and diminish inter-cell interference. The idea is that BSs act together as a single antenna array and users can receive their desired signals through BSs close to them. By choosing correctly the antenna outputs, interference can be minimized and the system capacity increased [14].

As a combination of massive MIMO, DAS architecture and CoMP technique, cell-free massive MIMO proposes that many randomly distributed APs are connected to a CPU and serve simultaneously a much smaller number of users. At the CPU, precoding techniques and power allocation algorithms can be performed. Compared to a cellular system, cell-free concepts have been shown to increase energy efficiency (EE) and per-user throughput, both in rural and urban scenarios [27].

The main challenges in its implementation are the need for a substantial backhaul overhead traffic, high deployment costs, and a sufficiently capable CPU. In particular, precoded signals and channel state information (CSI)

need to be shared among the base stations or APs [28]. Synchronization and feedback can also be cited as challenges brought by these technologies [29]. However, due to its ability to mitigate interference between cells, BSs/APs and users, cell-free can achieve significant gains in both the uplink and downlink.

2.1.2 Modulation and Propagation

Wireless systems require some fundamental definitions to convey information over the channel between the transmission and reception devices. In order to reach the other end in a communication system, transmit signals must be modulated and propagation effects analyzed.

The modulation process encodes a digital information signal into amplitude, phase, or frequency of the transmitted signal. The encoding process turns several bits into one symbol, and the rate of symbol transmission determines the bandwidth of the transmitted signal (the larger the number of bits per symbol, the greater the required received SNR for a given target BER) [30]. For mathematical simplicity, Quadrature Phase Shift Keying (QPSK) is used in this work. QPSK modulation consists of phase shift keying, changing the carrier phase at one or more points on the sine wave. In this type of modulation, the frequency and amplitude do not change, i.e., are kept constant [31]. In QPSK, two bits are modulated at once, mapping and selecting four possible carrier phase shifts (0, 90, 180, or 270 degrees) as its constellation diagram shows in Fig. 2.2.

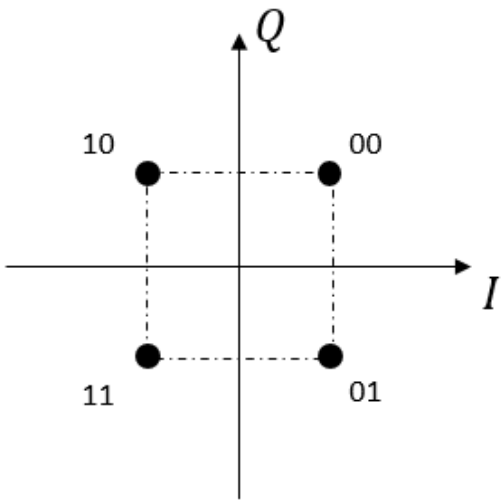

Figure 2.2: QPSK Gray Coded Constellation Diagram.

As previously mentioned, some propagation effects must be considered in wireless communication systems and are highlighted in this literature review.

Multi-path propagation creates an almost stationary fading pattern in space for each base station [32]. The line-of-sight (LOS) path can be considered as a transparent communication link over which data can be transmitted easily at very high speed, without delay spread. On the other hand, non-line-of-sight (NLOS) signals propagate everywhere causing delay spread in multi-path components and interference.

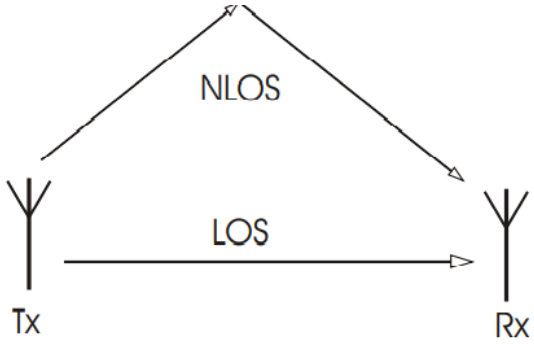

Figure 2.3: Difference between LOS and NLOS propagation.

Time variation and distance between the transmitter and the receiver causes fading on the received signal signal power. We will concentrate on large scaling fading which normally can be translated as significant modifications of the environment. We calculate large scale fading β, to be used in channel estimation, where m is the index that denotes an antenna element for MC and a specific AP in CF:

$$\beta_{m,k} = \mathrm{PL}_{m,k} \cdot 10^{\frac{\sigma_{sh} z_{m,k}}{10}}, \tag{2-1}$$

where σ_{sh} is the shadow fading standard deviation and $z_{m,k}$ is the shadowing coefficient:

$$\begin{aligned} \sigma_{sh} &= 8 \text{ dB}, \\ z_{m,k} &\sim \mathcal{N}(0,1). \end{aligned} \tag{2-2}$$

An obstacle between the transmitter and the receiver must be interpreted as parameters related to path loss and shadowing. For urban propagating scenario, we can calculate the path loss in dB (L) using COST-231 Hata method [33], represented below:

$$\begin{aligned} PL = {} & 46.3 + 33.9 log(f) - 13.82 log(h_m) \\ & - a(h_u) + (44.9 - 6.55 log(h_m)) log(d) + \mathrm{CM}. \end{aligned} \tag{2-3}$$

$1 \leq d \leq 20$km,

$1500 \leq f \leq 2000$ MHz,

$30 \leq h_{\mathrm{m}} \leq 200$ m,

$1 \leq h_{\mathrm{u}} \leq 10$ m,

CM= 3dB (correction factor for urban scenario),

$a(h_u) = 3.2(log(11.75h_u))^2 - 4.79$ (correction factor for the receiver antenna height in dB for urban scenarios),

f is the carrier frequency, h_{m} is the Tx antenna height, h_{u} is the user antenna height, and d is the distance between the antenna and the user.

For MC systems the COST 231 Hata model is used to calculate large scaling fading β, however its calculation is limited to the transmit antenna height between 30–200m. Considering that the antenna height in planned CF applications are $<$ 20m, this work adopts a different PL calculation which was presented in [34]:

$$\mathrm{PL}_{m,k} = \begin{cases} -L - 35\log_{10}(d_{m,k}), & \text{if } d_{m,k} > d_1 \\ -L - 15\log_{10}(d_1) - 20\log_{10}(d_{m,k}), & \text{if } d_0 < d_{m,k} \leq d_1 \\ -L - 15\log_{10}(d_1) - 20\log_{10}(d_0), & \text{if } d_{m,k} \leq d_0 \end{cases} \tag{2-4}$$

where

$$\begin{aligned} L &\triangleq 46.3 + 33.9\log_{10}(f) - 13.82\log_{10}(h_{\mathrm{AP}}) \\ &\quad - (1.1\log_{10}(f) - 0.7)\,h_{\mathrm{u}} + (1.56\log_{10}(f) - 0.8), \\ d_0 &= 10 \text{ m}, \\ d_1 &= 50 \text{ m}, \\ f &= 1900 \text{ MHz}, \\ h_{\mathrm{AP}} &= 15 \text{ m}, \\ h_{\mathrm{u}} &= 1.65 \text{ m}, \end{aligned} \tag{2-5}$$

For this CF scenario, h_{AP} is the AP antenna height in meters and $d_{m,k}$ is the distance between the mth antenna element and the kth user, as in [13]. When $d_{m,k} \leq d_1$ there is no shadowing.

2.1.3 MIMO Channel

The channel **H** can be modeled as a sum of dedicated LOS and NLOS propagation paths, and as some small changes in the user position causes significant changes in the phase of each multi-path component [32], we, therefore, can consider that channel the **H** is a sum of random variables. Since the number of multi-paths tends to infinity, we make use of central limit theorem and conclude that the entries of **H** follow a Gaussian distribution. We then present the system model for MIMO transmission:

$$\mathbf{y} = \mathbf{H}\mathbf{x} + \mathbf{w}; \tag{2-6}$$

In this work we focus on the study of DL transmission, where $\mathbf{y}$ is the vector of received samples $\mathbb{C}^{N_r \times 1}$, $\mathbf{x}$ is the vector of transmit signals $\mathbb{C}^{N_t \times 1}$, $\mathbf{w}$ is the vector of noise samples $\mathbb{C}^{N_r \times 1}$. The channel matrix $\mathbf{H}$ has dimensions given by $\mathbb{C}^{N_r \times N_t}$.

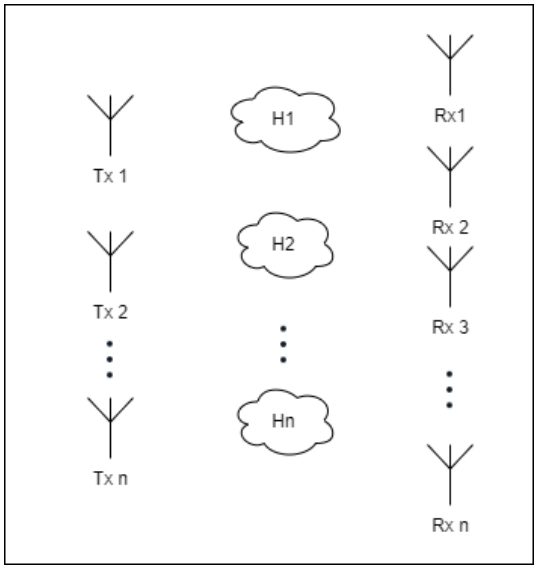

Figure 2.4: Channels in Multi User MIMO.

Mentioned before as a benefit of MIMO systems, spatial diversity, with a "massive" number of antennas at the base station, leads to channel hardening, which means that a fading channel behaves as if it was a non-fading channel. The randomness is still there but its impact on the communication is negligible.

2.1.3.1 Channel Capacity

Many advantages that we have pointed out in the previous sections include capacity gains, which increases the achievable information rates of the whole system. For point-to-point MIMO, since we have the cooperation

between users, we consider Claude Shannon's pioneering work in the late 1940s. His work showed that the capacity of a channel, defined to be the maximum rate at which reliable communication is possible, can be simply characterized in terms of the mutual information $I(X;Y)$ between the input and the output of the channel [4]:

$$I(X;Y) = \int_{Sx}\int_{Sy} f_x(x) f_{y|x}(y|x) \log_2\left(\frac{f_{y|x}(y|x)}{f_y(y)}\right) dydx, \tag{2-7}$$

where $f_x(x), f_y(y)$ and $f_{y|x}(y|x)$ are probability density functions.

It can also be written as function of differential entropy of channel output and conditional output:

$$I(X;Y) = h(Y)h(Y|X) = h(X)h(X|Y). \tag{2-8}$$

Finally, we obtain that the channel capacity of most channels is equal to the mutual information of the channel maximized over all possible input distributions, as shown by

$$C = \max_{p_x(x)} I(X;Y). \tag{2-9}$$

The differential entropies for $h(Y)$ and $h(X|Y)$ based on Gaussian vectors are computed along with the differential entropy for the Gaussian noise denoted as $\mathbf{w} \in \mathcal{NC}(O, \mathbf{C}_w)$, where $\mathbf{C}_w$ is the covariance matrix for the noise. As we already described in equation (2-6), we can perform the linear operation as $f_{y|x}(y|x) = f_w(yHx) = f_w(w)$, and $h(Y|X) = h(W)$, for the mutual information to hold:

$$I(X;Y) = h(Y) - h(W). \tag{2-10}$$

Computing the Gaussian distributed random process, applying logarithm rules, and considering that $\int_{Sm} f_w dw = 1$, the differential noise entropy is given by:

$$h(W) = \log_2(|\pi \mathbf{C}_w|) + \log_2(e)\mathrm{tr}(\mathbf{I}_{N_r}) = \log_2(|e\pi \mathbf{C}_w|)$$

and

$$h(Y) = \log_2(|e\pi \mathbf{C}_y|) = \log_2(|e\pi(\mathbf{C}_w + \mathbf{H}\mathbf{C}_x\mathbf{H}^H)|),$$

where $\mathbf{C}_x$ is the input covariance matrix, $\mathbf{C}_y$ is the output covariance matrix. Using Sylvester's determinant theorem [35], the mutual information yields:

$$I(X;Y) = \log_2(|\mathbf{I}_{N_t} + \mathbf{H}^H \mathbf{C}_n^{-1} \mathbf{H}\mathbf{C}_x|). \tag{2-11}$$

2.1.4 Uplink and Downlink

The channel from the users to the BS/AP is a multiple-access (MAC) or uplink (UL) channel, whereas the channel from the BS to the users is the broadcast channel (BC) or downlink (DL) channel [36]. We consider that the system has N_t antennas at the BS or AP, K users with N_r antennas and $\mathbf{H}_k$ denote the channel matrix for user k.

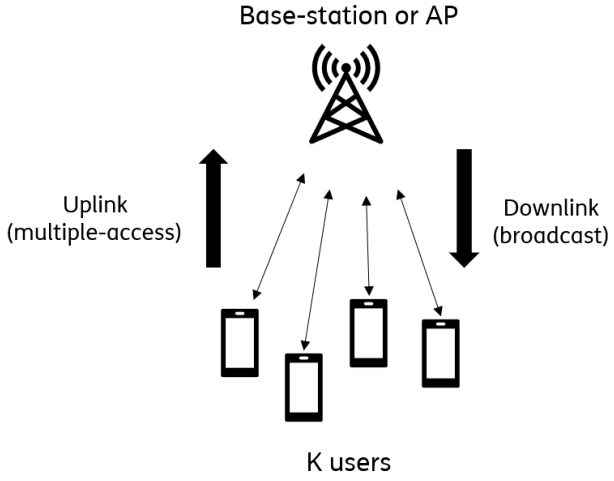

Figure 2.5: Uplink/downlink channels in wireless network systems.

In the UL, let $\mathbf{x}_k \in \mathbb{C}^{N_r \times 1}$ be the transmitted signal of user k. Let $\mathbf{y}^{UL} \in \mathbb{C}^{N_t \times 1}$ denote the received signal and $\mathbf{w} \in \mathbb{C}^{N_t \times 1}$ the noise vector, where $\mathbf{w} \sim \mathcal{CN}(O, \mathbf{C}_w)$ is a complex Gaussian with an identity covariance matrix sized by N_t. The received signal in the UL is given by

$$\begin{aligned} \mathbf{y}^{UL} &= \mathbf{H}_1^* \mathbf{x}_1 + \ldots + \mathbf{H}_K^* \mathbf{x}_K + \mathbf{w} \\ &= [\mathbf{H}_1^* \ldots \mathbf{H}_K^*] \begin{bmatrix} \mathbf{x}_1 \\ \vdots \\ \mathbf{x}_K \end{bmatrix} + \mathbf{w}. \end{aligned} \tag{2-12}$$

In the DL, $\mathbf{x} \in \mathbb{C}^{N_t \times 1}$ denotes the transmitted signal vector (from the BS/ AP) and $\mathbf{y}_k^{\mathrm{DL}} \in \mathbb{C}^{N_r \times 1}$ is the received signal at receiver k. The noise at receiver k is represented by $\mathbf{w}_k \in \mathbb{C}^{N_r \times 1}$ the noise vector and is assumed to be complex Gaussian noise $\mathbf{w}_k \sim \mathcal{CN}(O, \mathbf{C}_w)$. The received signal in the DL is given by

$$\mathbf{y}_k^{DL} = \mathbf{H}_k \mathbf{x} + \mathbf{w}_k. \tag{2-13}$$

In both links, each transmitter is assumed to have an independent data stream (an independent message for each of the receivers) and the capacity region is therefore a K-dimensional region.

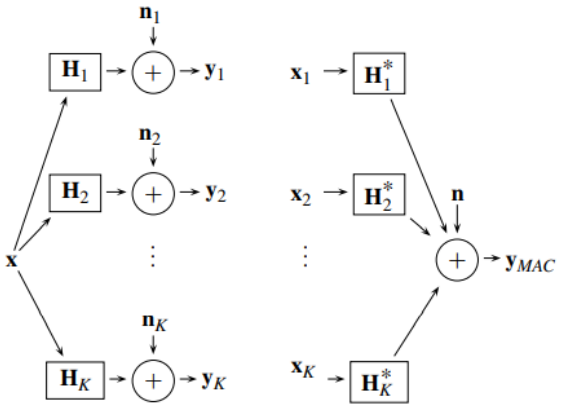

Figure 2.6: System models of MIMO DL (left) and the UL (right) channels.

For MIMO systems application, we normally use precoding techniques in the DL that will be discussed further on in this work and detection techniques in the UL. In this work, we focus on the design of linear precoders.

2.1.4.1 TDD protocol and Channel Estimation

For mathematical simplicity and channel reciprocity in the DL and UL, the system considers time-division duplex (TDD) for its duplex communication links. In the TDD protocol the data stream is divided into frames and carried over the same frequency by using different time slot to forward and reverse transmission. We separate the UL and DL signals by matching full duplex communication over a half-duplex communication link.

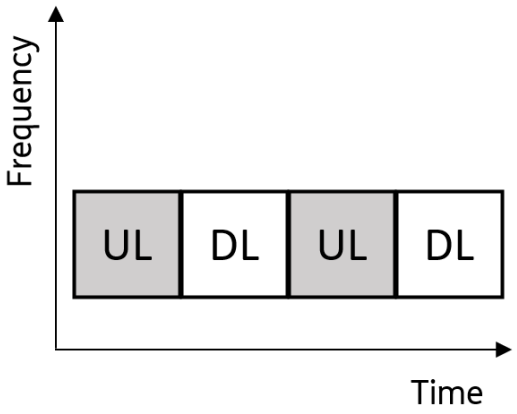

Figure 2.7: TDD Protocol.

Since the TDD protocol is assumed for full duplex communication, the channel is estimated through UL training and channel coefficients for the UL and DL are the same. We consider that channel state information (CSI) at the base station is obtained in the UL via users sending data. We can consider a few steps to estimate the channel in pilot-based scheme [32]:

i) Set a mathematical model to correlate the transmitted signal and the received signal using the channel matrix, presented in (2-6);

ii) User transmits a known signal as a pilot or as a training signal and BS detects the received signal;

iii) By comparing the transmitted signal and the received signal, we can figure out each element of the channel matrix $\mathbf{H}$;

iv) Data are transmitted back to the user that initiated the process.

We can represent a TDD protocol transmission in Fig. 2.8 for a coherent interval of time, using orthogonal frequency-division multiplexing (OFDM) modulation technique, which employs parallel transmission of orthogonal data in many carriers of different frequency with quadrature amplitude modulation (QAM) or PSK modulation, for QPSK symbols:

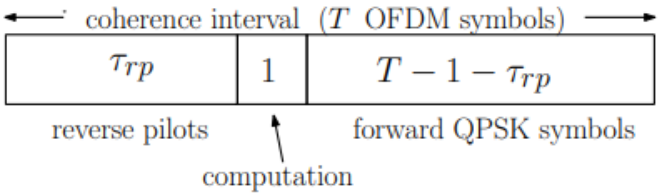

Figure 2.8: Transmission using TDD protocol

2.2 Downlink Precoding

In this section, we present the derivation of two DL linear precoders used in the this thesis: Conjugated Beamforming (CB)/ Matched Filter (MF) and Zero Forcing (ZF). Precoding techniques exploit channel information available at the transmitter (CSIT), therefore applied in DL to improve both the capacity and the error rate performance. We modify (2-6), where we can characterize the linear precoding matrix as $\mathbf{P}$. The estimate output signal $\tilde{\mathbf{x}}$ of the MIMO system is then given by:

$$\tilde{\mathbf{x}} = \mathbf{G}(\mathbf{HPx} + \mathbf{w}), \tag{2-14}$$

where $\mathbf{G}$ is a linear equalizer for point-to-point MIMO, however we consider as an identity matrix.

Linear precoding is known to provide an attractive trade-off between performance and computational complexity when causal CSIT is available in the form of channel estimates. Functionally, a linear precoder is a transmit operation matching the input signal covariance on one side and to the channel on the other. The structure is essentially a beamformer with single or multiple beams, each with a defined direction and power loading [4].

2.2.1 Conjugated Beamforming (CB) or Matched Filter (MF) Precoder

Our first precoder presented in this work, the CB has the objective to maximize signal-to-noise ratio at the receiver. It corresponds to the following optimization problem:

$$\begin{aligned} \mathbf{P}_{\mathrm{CB}} &= \arg\min \mathbb{E}\left\{\left|\left|\mathbf{x}^H\mathbf{GHPx}\right|\right|_2^2\right\} \\ s.t.\ \ &\mathrm{tr}(\mathbf{PC_xP^H}) = \mathrm{E_{tr}} \end{aligned} \tag{2-15}$$

Taking the derivative with respect to $\mathbf{P}^*$ from the Langragian function, we obtain:

$$L(\mathbf{P},\lambda) = \text{-tr}\{\mathbf{GHPC}_x\}\mathrm{tr}\{\mathbf{C}_x\mathbf{P}^H\mathbf{H}^H\mathbf{G}^H\} + \lambda(\mathrm{tr}\{\mathbf{PC}_x\mathbf{P}^H\} \text{ - Etr}) \tag{2-16}$$

$$\frac{\partial L(\mathbf{P},\lambda)}{\partial \mathbf{P}^*} = \text{- tr}\{\mathbf{GHPC}_x\}\mathbf{H}^H\mathbf{G}^H\mathbf{C}_x + \lambda\mathbf{PC}_x \tag{2-17}$$

Equating to zero and computing the transmit energy constraint, we have:

$$\mathbf{P}_{\mathrm{CB}} = \sqrt{\frac{\mathrm{E_{tr}}}{\mathrm{tr}\left\{\mathbf{H^HG}^H\mathbf{C}_x\mathbf{GH}\right\}}}\mathbf{H}^H\mathbf{G}^H \tag{2-18}$$

2.2.2 Zero Forcing Precoder

The Zero-Forcing signal transmitted to a user does not create interference to other users [36]. Its unbiased criterion is expressed by:

$$\mathbb{E}[f\tilde{\mathbf{x}}|\mathbf{x}] = \mathbf{x}$$
$$f\mathbf{GHPx} = \mathbf{x}$$
$$f\mathbf{GHP} = \mathbf{I}$$

It is an additional constraint to MMSE, as represented:

$$\begin{aligned} \mathbf{P}_{\mathrm{ZF}} &= \arg\min \mathbb{E}\left\{||\mathbf{x} - f\tilde{\mathbf{x}}||_2^2\right\} \\ &\text{s.t. } tr(\mathbf{P}\mathbf{C}_x\mathbf{P}^H) \leq \mathrm{E}_{\mathrm{tr}} \\ &\text{s.t. } f\mathbf{GHP} = \mathbf{I} \end{aligned} \tag{2-19}$$

When we assume that E_{tr} is the transmit energy:

$$\mathbf{P}_{\mathrm{ZF}} = \arg\min \mathbb{E}\left\{\left|\left|f - \mathbf{G}\mathbf{w}_2^2\right|\right|\right\}$$

The Lagrangian function is then given by:

$$\begin{aligned} L(\mathbf{P}, f, \mathbf{\Lambda}, \lambda) = f^2\mathrm{tr}\{\mathbf{GCwG}^H\} + \frac{1}{2}\,\mathrm{tr}\{\mathbf{\Lambda}(f\mathbf{GHP} - \mathbf{I})\} \\ + \frac{1}{2}\,\mathrm{tr}\{f\mathbf{H}^H\mathbf{G}^H\mathbf{\Lambda}^H\mathbf{P}^H\} - \frac{1}{2}\,\mathrm{tr}\{\mathbf{\Lambda}^H\} + \lambda(\mathrm{tr}\{\mathbf{PCxP}^H\} - \mathrm{E}_{\mathrm{tr}} \end{aligned} \tag{2-20}$$

Calculating with respect to $\mathbf{P}^*$ and equating it to zero:

$$\frac{\partial L(\mathbf{P}, f, \lambda)}{\partial \mathbf{P}^*} = \frac{1}{2}\mathbf{H}^{\mathrm{H}}\mathbf{G}^{\mathrm{H}}\mathbf{\Lambda}^{\mathrm{H}} + \lambda\mathbf{P}\mathbf{C}_{\mathbf{x}}$$

$$\mathbf{P} = \frac{-f}{2\lambda}\mathbf{H}^{\mathrm{H}}\mathbf{G}^{\mathrm{H}}\mathbf{\Lambda}^{\mathrm{H}}\mathbf{C}_{\mathbf{x}}^{-\mathbf{1}}$$

Finding values for $\mathbf{\Lambda}^H$ and using transmit energy constraint we find the following values:

$$\mathbf{P}_{\mathrm{ZF}} = \sqrt{\frac{\mathrm{E}_{\mathrm{tr}}}{\mathrm{tr}\left\{\mathbf{C}_{\mathbf{x}}(\mathbf{GHH}^{\mathrm{H}}\mathbf{G}^{\mathrm{H}})^{-1}\right\}}}\mathbf{H}^{\mathrm{H}}\mathbf{G}^{\mathrm{H}}(\mathbf{GHH}^{\mathrm{H}}\mathbf{G}^{\mathrm{H}})^{-\mathbf{1}} \tag{2-21}$$

with transmit energy constraint:

$$f = \sqrt{\frac{\mathrm{tr}\left\{\mathbf{C_x}(\mathbf{GHH}^{\mathrm{H}}\mathbf{G}^{\mathrm{H}})^{-1}\right\}}{\mathrm{E_{tr}}}} \tag{2-22}$$

2.3 Downlink Power Allocation

In every system design, system capacity is taken into account. Considering the expression that we derive in (2-11), the downlink achievable rate of user k is R_k, assuming Gaussian signaling, is represented below:

$$R_k = \log_2(1 + \mathrm{SINR}_k). \tag{2-23}$$

With m being the index that denotes the m-th transmit antenna, the transmitted signal follows:

$$x_m = \rho_f \sum_{i=1}^{K} \sqrt{\eta_{mi}} h_{mi} s_i. \tag{2-24}$$

For simplicity, note a difference between CF and MC for channel $h = \hat{h}^*_{cf} = h_{mc}$ (see in details in Section 2.4). ρ_f is the maximum transmitted power of each antenna in the transmitter, η_{mi} is the power coefficient used by the transmit antenna m to user i, The quantity h_{mi} is the channel coefficient between m and i, $\tilde{h}_{mi}$ is the estimation of the channel coefficient and s_i is the symbol intended for user i with $\mathbb{E}\left(|s_i|^2\right) = 1$.
The signal received by user k is

$$y_k = \sum_{m=1}^{M} h_{mk} x_m + w_k \tag{2-25}$$

where $w_k \sim \mathcal{CN}(0, 1)$ is additive noise.

We now find the derivation for capacity lower bound in (2-25):

$$\begin{aligned} y_k = & \underbrace{\sum_{m=1}^{M} \sqrt{\rho_f\ \eta_{mk}}\ \mathbb{E}\left(|h_{mk}|^2\right) s_k}_{T_0\text{: desired signal}} + \underbrace{\sum_{m=1}^{M} \sum i \neq k^K \sqrt{\rho_f\ \eta_{mi}}\ h_{mk} s_i}_{T_1\text{: interference}} \\ & + \underbrace{\sum_{m=1}^{M} \sqrt{\rho_f\ \eta_{mk}} \left(|h_{mk}|^2 - \mathbb{E}\left(|h_{mk}|^2\right)\right) s_k}_{T_2\text{: lack of channel knowledge at user}} \\ & + \underbrace{\sum_{m=1}^{M} \sum_{i=1}^{K} \sqrt{\rho_f\ \eta_{mi}}\ \tilde{h}_{mk}\ h_{mk} s_i}_{T3\text{: channel estimation error}} + w_k \end{aligned} \tag{2-26}$$

Assuming that the data signals for different users are uncorrelated and

w_k is statistically independent from data signals and channel coefficients, one can check T_0, T_1, T_2, T_3 and w_k are mutually uncorrelated.

Hence, SINR_k is given by

$$\mathrm{SINR}_k = \frac{\mathbb{E}\left(|T_0|^2\right)}{\sigma_w^2 + \mathbb{E}\left(|T_1|^2 + |T_2|^2 + |T_3|^2\right)} \tag{2-27}$$

where:

$$\begin{aligned}
\mathbb{E}\left(|T_0|^2\right) &= \rho_f \left(\sum_{m=1}^{M} \sqrt{\eta_{mk}}\alpha_{mk}\right)^2 \\
\mathbb{E}\left(|T_1|^2\right) &= \rho_f \sum_{i\neq k}^{K}\sum_{m=1}^{M} \eta_{mi}\alpha_{mk}\alpha_{mi} \\
\mathbb{E}\left(|T_2|^2\right) &= \rho_f \sum_{m=1}^{M} \eta_{mk}\alpha_{mk}^2 \\
\mathbb{E}\left(|T_3|^2\right) &= \rho_f \sum_{i=1}^{K}\sum_{m=1}^{M} \eta_{mi}\left(\beta_{mk} - \alpha_{mk}\right)\alpha_{mi}
\end{aligned}$$

The results lead us to a new expression for (2-23) in each precoder design. In the system model presented in (2-6) (already modified by precoding matrix $\mathbf{P}$ explained in Section 2.2), we introduce $\mathbf{N}$ as the power allocation matrix. Instead of having entries $\eta_{m,k}$, $\mathbf{N}$ will be a diagonal matrix where its coefficients are only function of k, such as $\eta_{m,k} = \eta_k,\ k = 1, \ldots, K$. Then, $\mathbf{N}$ is a diagonal matrix with $\sqrt{\eta_1}, \ldots, \sqrt{\eta_K}$ on its diagonal:

$$\mathbf{N} = \begin{bmatrix} \sqrt{\eta_1} & 0 & \ldots & 0 \\ 0 & \sqrt{\eta_2} & \ldots & 0 \\ \vdots & \vdots & \ddots & \vdots \\ 0 & 0 & \ldots & \sqrt{\eta_k} \end{bmatrix} \tag{2-28}$$

The received signal for all users $\mathbf{y} \in \mathbb{C}^{N_r \times 1}$ is then:

$$\mathbf{y} = \sqrt{\rho_f}\ \mathbf{HPNs} + \mathbf{w}. \tag{2-29}$$

where ρ_f is the transmit power limit, the channel matrix $\mathbf{H} \in \mathbb{C}^{N_r \times N_t}$, the precoding matrix $\mathbf{P} \in \mathbb{C}^{N_t \times N_r}$, the power allocation matrix $\mathbf{N} \in \mathbb{C}^{N_r \times N_r}$, the symbol vector $\mathbf{s} \in \mathbb{C}^{N_r \times 1}$, and the noise vector $\mathbf{w} \in \mathbb{C}^{N_r \times 1}$.

2.4 System Models

During the first section of this work, we have presented a literature review on Massive MIMO, signal propagation, MIMO channel capacity, UL and DL system models, and also DL precoding and power allocation. Those characteristics are present for both MIMO architectures presented below.

In this section, we will highlight the behavior and elements that are essential for cellular and cell-free systems. Furthermore, we will point out the main differences, aiming the presentation of the numerical results.

2.4.1 Multi-Cell Systems

Introduced to amplify system capacity by the frequency reuse technique, the cellular concept has become essential for wireless cellular systems. The method collaborates to the increase the number of available channels, consequently the number of users in the system [37], and avoid interference. A cellular network is characterized by centralized communication where multiple users within a cell communicate with a base-station that controls all transmission/reception and forwards data to the users [4]. The base-station is located at the center of each cell and a set of cells form a cluster Fig. 2.9. This architecture represents the CAS topology for MIMO systems.

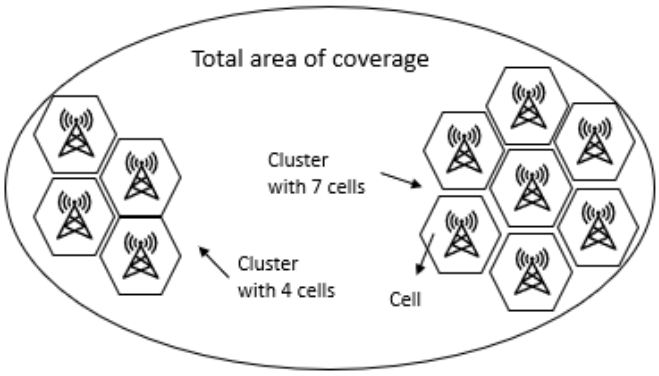

Figure 2.9: Multi cellular system concept.

The most used cell geometry is hexagonal cells due to uniformity in levels of interference between cells using the same set of channels in different clusters (co-cells), since they have the same distance of reuse D for all neighbor clusters [38]. In tentative to cover the largest area and serve the maximum number of users as possible, cellular systems are formed by many clusters. To calculate the area of each cell a and the area of the cluster A, we have:

$$a = 3\sqrt{3}\frac{R^2}{2} \text{ and } A = \sqrt{3}\frac{D^2}{2}, \tag{2-30}$$

where D is the distance between co-cells for frequency channel reuse and R is the radius of the cell. We use the results to calculate Q, the number of cells in a cluster (meaning the number of sub-channels that we divide the total of available channels in a cluster) and reuse factor q as below:

$$Q = \frac{A}{a} = \frac{D^2}{3R^2} \tag{2-31}$$

The distance of reuse is:

$$\begin{aligned} D &= \sqrt{i^2 + ij + j^2}\sqrt{3R^2} \\ Q &= \sqrt{i^2 + ij + j^2} \\ q &= \frac{D}{R} = \sqrt{3Q} \end{aligned} \tag{2-32}$$

Even though the system diminish channel frequency interference ensuring that cells with the same carrier frequency keep distance between co-cells D [39], network stills suffer with inter-cell interference (ICI) and performance drastically decreases when users are at cell-edge due to the distance to the BS (see subsection 2.1.2).

Considering the CAS setup explained connected to a Core Network (CN) through a backhaul for signaling, we describe a mathematical model for this MIMO DL transmission for all the users in a cell as we explained in (2-35).

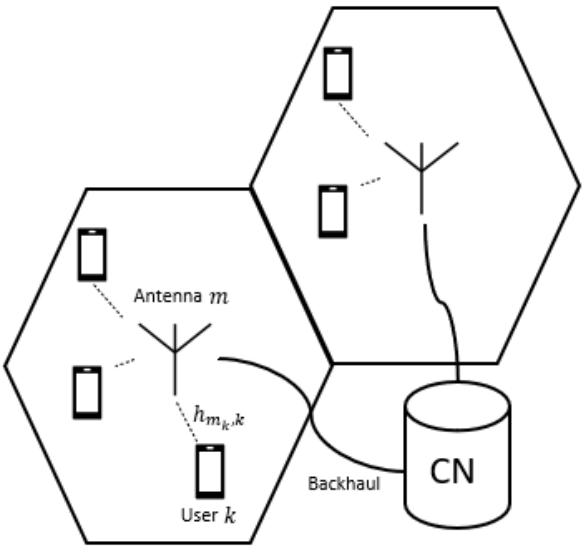

Figure 2.10: Multi-Cellular Massive MIMO System.

Assume that all users K in the cell are served by only one BS with M antennas. For antenna assignment, we take a greedy solution and choose the antenna with the largest large-scale fading coefficient ($\beta_{m_k,k}$):

$$m_k = \text{ argmax } \beta_{mk} \tag{2-33}$$

Channel estimation is performed by pilot-based scheme, to obtain the channel matrix $\mathbf{H}$. We can consider the received symbol for the k-th user:

$$y_k = \underbrace{\sqrt{\rho_f} h_{k,m} p_{m,k} n_{k,k} s_k}_{\text{desired signal}} + \underbrace{\sqrt{\rho_f} \sum_{\substack{j=1 \\ j \neq k}}^{K} h_{k,m} p_{m,j} n_{j,j} s_j}_{\text{other users interference}} + \underbrace{w_k}_{\text{noise}} \tag{2-34}$$

For all users in a cell c, the received signal $\mathbf{y}_c$ is then:

$$\mathbf{y}_c = \sqrt{\rho_f}\ \mathbf{H}_{MC}\mathbf{PNs} + \mathbf{w}. \tag{2-35}$$

where $\mathbf{y}_c \in \mathbb{C}^{K\times 1}$, ρ_f is the transmit power limit, the channel matrix $\mathbf{H}_{MC} \in \mathbb{C}^{K\times M}$, the precoding matrix $\mathbf{P} \in \mathbb{C}^{M\times K}$, the power allocation matrix $\mathbf{N} \in \mathbb{C}^{K\times K}$, the symbol vector $\mathbf{s} \in \mathbb{C}^{K\times 1}$, and the noise vector $\mathbf{w} \in \mathbb{C}^{K\times 1}$.

In the simulations developed in this work, we have considered systems with M transmit antennas and K receive antennas communicating using Rayleigh fading channel in each cell. The MC system with $C = 4$ and QPSK modulation was introduced to encode the symbols. Three linear precoding techniques, MF or CB, ZF and MMSE, were compared during the simulations. We also considered and compared three power allocation techniques, namely, UPA, APA and R-APA for this system.

2.4.2 Cell-Free Systems

Cell-free (CF) massive MIMO systems have a large number of individually controllable low-cost low-power single antenna access point (APs) distributed over a wide area for simultaneously serving a small number of user equipments (UEs) [15]. We have consider a DAS MIMO topology for this work.

The APs are connected via backhaul network to a Central Processing Unit (CPU) and serve all users in the same time-frequency resource via TDD. Each AP obtains CSI by UL and sends them to the CPU, which performs AP selection (APS), precoding and power allocation whose parameters are then fed back to the APs [40]. This framework brings about the two fold benefits of having a reduced data payload in the fronthaul and an increased SE for all

UEs [8]. However, when compared to CAS, cell-free has much more backhaul complexity, since the communication between payload data, and power control coefficients is done in the CPU.

Assuming that the users are surrounded by APs, all UEs may have good channel conditions.

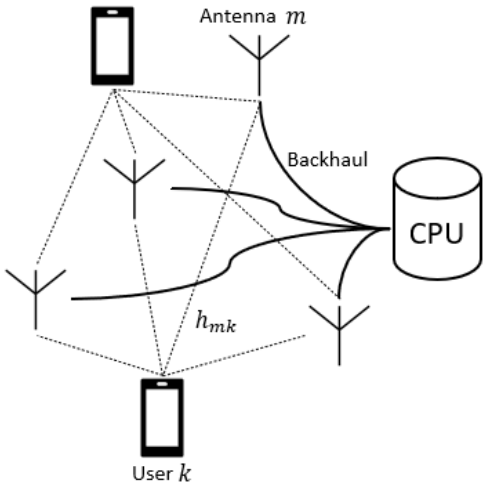

Figure 2.11: Cell-Free Massive MIMO System.

In order to avoid short symbols intervals and lose coherence interval, the applications of CF structure is considered for scenarios where the mobility of the users are less than 10 km/h. Smart factory, train stations, small villages, shopping malls, stadiums, subways, hospitals, community centers and/or a college campus would be some examples for indoors and/or hot-spots schemes that would have great coverage.

We consider a Cell-Free Massive MIMO system with M APs and K users, where $M >> K$. The channel coefficient between the AP m and user k is represented below:

$$h_{mk} = \sqrt{\beta_{mk}} g_{mk}, \tag{2-36}$$

where β_{mk} is the large scale fading coefficient which accounts pathloss and shadowing effects. The small scale fading coefficient $g_{mk} \sim \mathcal{CN}(0, 1)$.

We assume that these coefficients are i.i.d random variables that remain constant during a coherent interval and are independent in different intervals. We denote the channel matrix between all APs and users by $\mathbf{H} \in \mathbb{C}^{M \times K}$.

To reduce interference in the TDD protocol, it is required channel estimation and we can consider UL pilot-scheme.

As the first step of the protocol, all users simultaneously and synchronously transmit reverse orthonormal pilots sequences $\{\psi_1, \ldots, \psi_K\} \in \mathbb{C}^{\tau}$,

which propagate to all M APs. Then, APs perform channel estimation, obtaining estimates $\hat{h}_{mk}$ of h_{mk}. This technique can result in pilot contamination, however we assume that the coherence intervals are large such that the pilot contamination is negligible (users with the same pilot are located far from each other).

As a final step of the protocol, all APs get estimates of the channel coefficients and use this info to transmit data to all users. It is considered orthogonal pilots.

The received signal sequence in the training step at AP m is:

$$y_m = \sqrt{\rho_f \tau} \sum_{i=1}^{K} h_{mi} \psi_i + w_m, \tag{2-37}$$

where ρ_f is the maximum transmitted power of each user, $w_m \sim \mathcal{CN}(0, I_\tau)$ is additive noise and τ is the length of pilot sequences, in this case, $\tau = K$.

The AP computes the following estimation:

$$\hat{g}_{mk} = \frac{\sqrt{\rho_f \tau}\beta_{mk}}{1 + \rho_r \tau \beta_{mk}} \psi_k^H y_m. \tag{2-38}$$

Due to channel hardening in Massive MIMO systems cited in section 1, we assume that each user is only aware of the statistics of the estimated channel coefficients. Then, the variance of this estimate, $\mathbb{E}\left(|\hat{g}_{mk}|^2\right)$, is given by:

$$\alpha_{mk} = \frac{\rho_r \tau \beta_{mk}^2}{1 + \rho_r \tau \beta_{mk}} \tag{2-39}$$

Let the channel estimation error be:

$$\tilde{g}_{mk} = g_{mk} - \hat{g}_{mk} \tag{2-40}$$

where

$$\hat{g}_{mk} \sim \mathcal{CN}(0, \alpha_{mk})$$
$$\tilde{g}_{mk} \sim \mathcal{CN}(0, \beta_{mk}\alpha_{mk})$$

We consider channel reciprocity explained in the literature review, meaning that channel coefficients are the same for DL and UL. After channel estimation, we can consider the data transmitted to K users in DL, so that m-th AP transmits the symbols:

$$x_m = \sqrt{\rho_f} \sum_{k=1}^{K} p_{mk} a_{mk} s_k, \tag{2-41}$$

where ρ_f is the transmit power limit of each antenna, p_{mk} is the precoding coefficient and a_{mk} is the power coefficient used by AP m for transmission to user k, and s_k is the data signal intended for user k.

The signal received by the k-th user is then represented by:

$$y_k = \sum_{m=1}^{M} h_{mk} x_m + w_k, \tag{2-42}$$

where $w_k \sim CN(0, \sigma_w^2)$.

For all APs combined we can express the trasnmitted vector as $\mathbf{x} = \mathbf{PNs}$. For all users, we express the received vector:

$$\mathbf{y}_{CF} = \sqrt{\rho_f}\mathbf{H}_{CF}^T\mathbf{x} + \mathbf{w}, \tag{2-43}$$

where in this framework, the channel matrix $\mathbf{H}_{CF} \in \mathbb{C}^{M\times K}$, $\mathbf{P} \in \mathbb{C}^{M\times K}$ is the precoding matrix, $\mathbf{N} \in \mathbb{C}^{K\times K}$ is the power allocation matrix, then $\mathbf{s}$ and $\mathbf{w} \in \mathbb{C}^K$ are the symbol and noise vectors, respectively. Note a small difference between dimensions in $\mathbf{H}_{CF}$ and $\mathbf{H}_{MC}$ (presented before), however $\mathbf{y}_{CF} \in \mathbb{C}^{K\times 1}$ and $\mathbf{y}_{MC}$ have the same dimensions.

In simulations, we compare some DL Precoders (CB, ZF and MMSE) and power allocation techniques (UPA, APA and R-APA) in terms of Sum Rate vs SNR and BER vs SNR for this system model. Previous works has shown that CF systems provide five to ten fold improvement in 95% per user throughput when compared to Small Cells with $m = 1$ [15] and [13], however this works considers a MC system with 4 cells cluster with MIMO increasing the number of transmitters per cell.

2.5 Numerical Results

In Fig. 2.12 we analyze the numerical results of all techniques explained in this chapter. First, we present a MIMO transmission for K=4 and M=8, in only one cell with ZF and CB precoders. For math simplicity, the simulation was performed using QPSK modulation, UPA technique, and considered Rayleigh fading channel. We used 120 channel realizations and 100 transmitted symbols for each transmission. We clearly notice a much better performance obtained with the ZF precoder, where in very low SNR rates accomplished no more bit errors (achieved 0 BER at 10 dB). We can also highlight that CB stays constant close to 10^{-3}. In both schemes, the results are excellent, with rates very close to 0 for very low SNR.

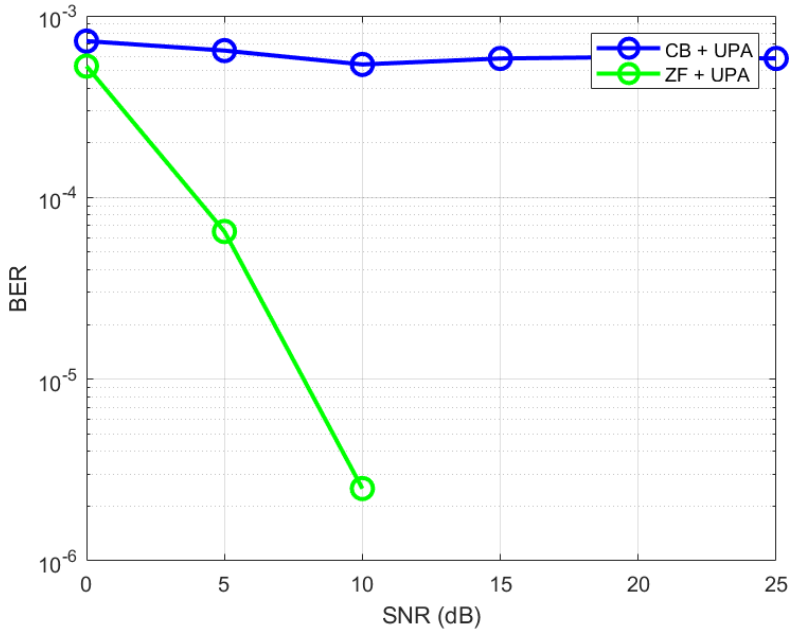

Figure 2.12: System Performance: One-Cell with K = 4 and M = 8.

Next, we apply the DL linear precoding and power allocation techniques previously described to the two system architectures that we discussed in Section 2.4. We observe that in general the ZF precoder has the best performance overall. MC + ZF achieved better rates for the proposed setup, with less than 10^{-1} after 13 dB. Furthermore, MC with CB and CF with CB remained almost constant.

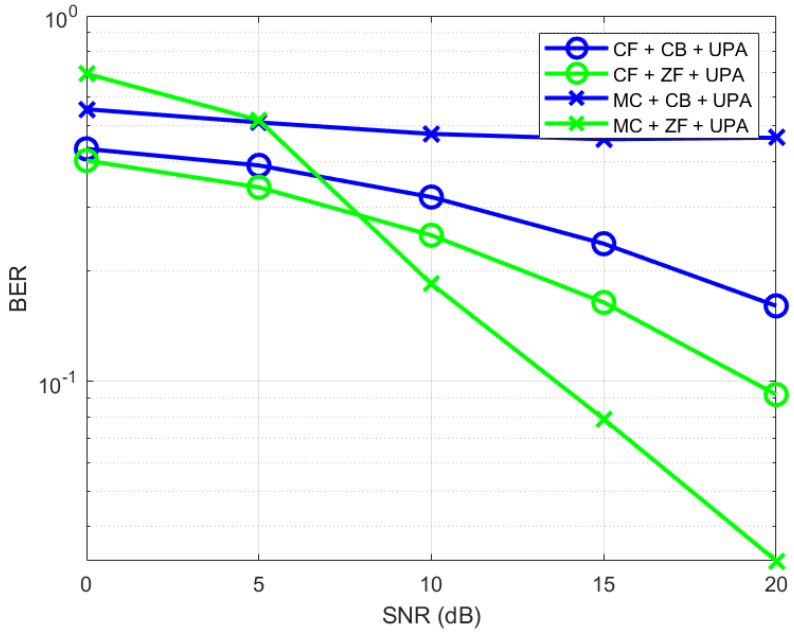

Figure 2.13: System Performance: Multi-Cell with C=4, K=1 per cell and M=8 vs Cell-Free with K=4 and M=32.

In this chapter, we have presented some literature review on MIMO system, including modulation and propagation overview, MIMO channel explanation and capacity calculation, uplink and downlink models, downlink precoder designs, power allocation details and two different system architecture schemes.

3
MMSE Precoding and Power Allocation for Multi-Cell and Cell-Free Massive MIMO Systems

In this chapter, we detail the derivation of the linear MMSE precoder for the downlink and the adaptive power allocation schemes based on max-min fairness for this specific precoder.

In Section 3.1, we provide the derivation of the MMSE precoder with total power constraint. In Section 3.2 we calculate the power coefficients to maximize the SINR in order to achieve good information rates. The UPA restriction is used and we also show two other adaptive algorithms to improve the performance of the systems. In both adaptive approaches, the MSE cost function is used to recalculate $\mathbf{N}$. In Section 3.3, we study the computational complexity of precoders and power allocation techniques presented in this work. Finally, numerical results are presented and individually analyzed for the developed schemes and applied to CF and MC settings.

3.1
Linear MMSE Precoder

Let us focus on the derivation of the linear MMSE precoder, which has proven to have better performance than the linear ZF precoder for both CF and MC [15].

The linear MMSE precoder includes a total transmit power constraint in the form of an inequality [41]. At the receiver, the received signal will be scaled, for example, with an automatic gain control f. This kind of scaling is relevant for the MSE and therefore it is taken into account in the optimization problem and in the precoder design.

By taking into account the expression in (2-35), we start the derivation:

$$\mathbf{y} = \sqrt{\rho_f}\,\mathbf{HPNs} + \mathbf{w}. \tag{3-1}$$

For simplification purposes, we assume that the derivation is valid for MC and CF system, however notations of variables $\mathbf{P}$, $\mathbf{H}$ and $\mathbf{N}$ are different in each of these systems.

We consider that the linear precoder matrix $\mathbf{P}_{MMSE}$ corresponds to the solution of the following optimization problem:

$$\begin{aligned} \mathbf{P}_{MMSE} &= \arg\min \mathbb{E}\{|\mathbf{s} - f\mathbf{y}|_2^2\} \\ s.t.\ &\mathbb{E}\left[\|\mathbf{x}\|_2^2\right] \leq \mathrm{E}_{\mathrm{tr}}, \end{aligned} \tag{3-2}$$

where the transmit signal is given by

$$\mathbf{x} = \sqrt{\rho_f}\mathbf{PNs} \tag{3-3}$$

The average transmit power is obtained through

$$\begin{aligned} \mathbb{E}\left[\|\mathbf{x}\|_2^2\right] &= \mathbb{E}\left[\left(\sqrt{\rho_f}\mathbf{PNs}\right)^H \left(\sqrt{\rho_f}\mathbf{PNs}\right)\right] \\ &= \rho_f \mathbb{E}\left[\mathbf{s}^H\mathbf{N}^H\mathbf{P}^H\mathbf{PNs}\right] \\ &= \rho_f \mathrm{tr}\left(\mathbb{E}\left[\mathbf{s}^H\mathbf{N}^H\mathbf{P}^H\mathbf{PNs}\right]\right) \\ &= \rho_f \mathbb{E}\left[\mathrm{tr}\left(\mathbf{N}^H\mathbf{P}^H\mathbf{PNss}^H\right)\right] \\ &= \rho_f \mathrm{tr}\left(\mathbf{PNC}_s\mathbf{N}^H\mathbf{P}^H\right) = \mathrm{E}_{\mathrm{tr}}, \end{aligned} \tag{3-4}$$

where E_{tr} denotes the total transmit power constraint, and $\mathbb{E}[\mathbf{ss}^H] = \mathbf{C}_s$ is the covariance matrix of $\mathbf{s}$. Because the transmit energy is constrained, it is considered that the received signal is scaled with factor f at the receiver, which is part of the optimization. The design of the precoder matrix $\mathbf{P}_{MMSE}$ is constrained as follows:

$$\begin{aligned} \mathbf{P}_{MMSE} &= \arg\min \mathbb{E}\{|\mathbf{s} - f\mathbf{y}|_2^2\} \\ s.t.\ &\rho_f \mathrm{tr}(\mathbf{PNC_sN^HP^H}) \leq \mathrm{E}_{\mathrm{tr}}, \end{aligned} \tag{3-5}$$

The MSE cost function is then described as:

$$\begin{aligned} \mathcal{C}(\mathbf{N}) = \mathbb{E}\left[\|\mathbf{s} - f\mathbf{y}\|_2^2\right] &= \mathbb{E}\left[(\mathbf{s} - f\mathbf{y})^H(\mathbf{s} - f\mathbf{y})\right] \\ &= \mathbb{E}\left[\mathbf{s}^H\mathbf{s} - f\mathbf{s}^H\mathbf{y} - f\mathbf{y}^H\mathbf{s} + f^2\mathbf{y}^H\mathbf{y}\right] \\ &= \mathbb{E}\Big[\mathbf{s}^H\mathbf{s} - f\mathbf{s}^H\left(\sqrt{\rho_f}\mathbf{HPNs} + \mathbf{w}\right) \\ &\quad - f\left(\sqrt{\rho_f}\mathbf{HPNs} + \mathbf{w}\right)^H\mathbf{s} \\ &\quad + f^2\left(\sqrt{\rho_f}\mathbf{HPNs} + \mathbf{w}\right)^H\left(\sqrt{\rho_f}\mathbf{HPNs} + \mathbf{w}\right)\Big] \end{aligned} \tag{3-6}$$

We can highlight a small difference from CF to MC at this point of derivation, where $\mathbf{H}_{\mathrm{cf}}^T$ and $\mathbf{H}_{\mathrm{mc}}$ have different dimensions. Even though $(\mathbf{H}_{\mathrm{cf}}^T)^H = \mathbf{H}_{\mathrm{cf}}^*$ and $\mathbf{H}_{\mathrm{mc}}^H$, the calculation can be simplified with $\mathbf{H}_{\mathrm{cf}}^T = \mathbf{H}_{\mathrm{mc}} = \mathbf{H}$ as demonstrate in (2-35), meeting the compatibility of dimensions for each system and its variables with the explanation above. By using the properties of the expected value operator, we have:

$$
\begin{aligned}
&= \mathbb{E}\left[\mathbf{s}^H\mathbf{s}\right] - f\mathbb{E}\left[\sqrt{\rho_f}\mathbf{s}^H\mathbf{HPNs}\right] - f\mathbb{E}\left[\mathbf{s}^H\mathbf{w}\right] \\
&\quad - f\mathbb{E}\left[\sqrt{\rho_f}\mathbf{s}^H\mathbf{N}^H\mathbf{P}^H\mathbf{H}^H\mathbf{s}\right] - f\mathbb{E}\left[\mathbf{w}^H\mathbf{s}\right] \\
&\quad + f^2\mathbb{E}\left[\rho_f\mathbf{s}^H\mathbf{N}^H\mathbf{P}^H\mathbf{H}^H\mathbf{HPNs}\right] \\
&\quad + f^2\mathbb{E}\left[\sqrt{\rho_f}\mathbf{s}^H\mathbf{N}^H\mathbf{P}^H\mathbf{H}^H\mathbf{w}\right] + f^2\mathbb{E}\left[\sqrt{\rho_f}\mathbf{w}^H\mathbf{HPNs}\right] \\
&\quad + f^2\mathbb{E}\left[\mathbf{w}^H\mathbf{w}\right].
\end{aligned} \tag{3-7}
$$

Data symbols and the noise are statistically independent, leading to $\mathbb{E}[\mathbf{s}\mathbf{w}^H] = 0$ and $\mathbb{E}[\mathbf{s}^H\mathbf{w}] = 0$:

$$
\begin{aligned}
\mathbb{E}\left[\|\mathbf{s} - f\mathbf{y}\|_2^2\right] &= \mathbb{E}\left[\mathbf{s}^H\mathbf{s}\right] - f\sqrt{\rho_f}\mathbb{E}\left[\mathbf{s}^H\mathbf{HPNs}\right] \\
&\quad - f\sqrt{\rho_f}\mathbb{E}\left[\mathbf{s}^H\mathbf{N}^H\mathbf{P}^H\mathbf{H}^H\mathbf{s}\right] \\
&\quad + f^2\rho_f\mathbb{E}\left[\mathbf{s}^H\mathbf{N}^H\mathbf{P}^H\mathbf{H}^H\mathbf{HPNs}\right] + f^2\mathbb{E}\left[\mathbf{w}^H\mathbf{w}\right].
\end{aligned} \tag{3-8}
$$

Applying the trace operator and considering $\mathbb{E}[\mathbf{s}\mathbf{s}^H] = \mathbf{C}_s$ and $\mathbb{E}[\mathbf{w}\mathbf{w}^H] = \mathbf{C}_w$, where $\mathbf{C}_w$ is the noise covariance matrix:

$$
\begin{aligned}
\mathbb{E}\left[\|\mathbf{s} - f\mathbf{y}\|_2^2\right] &= \mathrm{tr}\left(\mathbf{C}_s\right) - f\sqrt{\rho_f}\mathrm{tr}\left(\mathbf{HPNC}_s\right) \\
&\quad - f\sqrt{\rho_f}\mathrm{tr}\left(\mathbf{N}^H\mathbf{P}^H\mathbf{H}^H\mathbf{C}_s\right) \\
&\quad + f^2\rho_f\mathrm{tr}(\mathbf{N}^H\mathbf{P}^H\mathbf{H}^H\mathbf{HPNC}_s) + f^2\mathrm{tr}\left(\mathbf{C}_w\right),
\end{aligned} \tag{3-9}
$$

The Lagrangian function can be written taking into account the power constraint in (3-5), with the Lagrange multiplier λ and setting its derivative to zero:

$$
\begin{aligned}
\mathcal{L}\left(\mathbf{P}, f, \lambda\right) = &\ \mathbb{E}\left[\|\mathbf{s} - f\mathbf{y}\|_2^2\right] + \lambda\left(\rho_f\mathrm{tr}\left(\mathbf{PNC}_s\mathbf{N}^H\mathbf{P}^H\right) - \mathrm{E}_{\mathrm{tr}}\right) \\
&= \mathrm{tr}\left(\mathbf{C}_s\right) - f\sqrt{\rho_f}\mathrm{tr}\left(\mathbf{HPNC}_s\right) \\
&\quad - f\sqrt{\rho_f}\mathrm{tr}\left(\mathbf{H}^H\mathbf{C}_s\mathbf{N}^H\mathbf{P}^H\right) \\
&\quad + f^2\rho_f\mathrm{tr}\left(\mathbf{H}^H\mathbf{HPNC}_s\mathbf{N}^H\mathbf{P}^H\right) + f^2\mathrm{tr}\left(\mathbf{C}_w\right) \\
&\quad + \lambda\left(\rho_f\mathrm{tr}\left(\mathbf{PNC}_s\mathbf{N}^H\mathbf{P}^H\right) - \mathrm{E}_{\mathrm{tr}}\right).
\end{aligned} \tag{3-10}
$$

Using Wirtinger's calculus where $\partial\mathrm{tr}\left(\mathbf{AB}^H\right)/\partial\mathbf{B}^* = \mathbf{A}$, with respect to $\mathbf{P}^*$ we have:

$$
\begin{aligned}
\frac{\partial\mathcal{L}\left(\mathbf{P}, \mathbf{N}, f, \lambda\right)}{\partial\mathbf{P}^*} &= f^2\rho_f\mathbf{H}^H\mathbf{HPNC}_s\mathbf{N}^H + \lambda\rho_f\mathbf{PNC}_s\mathbf{N}^H \\
&\quad - f\sqrt{\rho_f}\mathbf{H}^H\mathbf{C}_s\mathbf{N}^H = 0,
\end{aligned} \tag{3-11}
$$

We then solve (3-11):

$$
\begin{aligned}
&f^2\rho_f\mathbf{H}^H\mathbf{H}\mathbf{P}\mathbf{N}\mathbf{C}_s\mathbf{N}^H + \lambda\rho_f\mathbf{P}\mathbf{N}\mathbf{C}_s\mathbf{N}^H - f\sqrt{\rho_f}\mathbf{H}^H\mathbf{C}_s\mathbf{N}^H = 0\\
&f\sqrt{\rho_f}\mathbf{H}^H\mathbf{C}_s\mathbf{N}^H = \rho_f\mathbf{H}^H\mathbf{H}\mathbf{P}\mathbf{N}\mathbf{C}_s\mathbf{N}^H + \lambda f^2\rho_f\mathbf{P}\mathbf{N}\mathbf{C}_s\mathbf{N}^H\\
&f\sqrt{\rho_f}\mathbf{H}^H = \rho_f\mathbf{H}^H\mathbf{H}\mathbf{P}\mathbf{N} + \lambda f^2\rho_f\mathbf{P}\mathbf{N}\\
&f\sqrt{\rho_f}\mathbf{H}^H = \rho_f\left(\mathbf{H}^H\mathbf{H} + \lambda f^2\mathbf{I}_M\right)\mathbf{P}\mathbf{N}\\
&\mathbf{P}\mathbf{N} = \frac{f}{\sqrt{\rho_f}}\underbrace{\left(\mathbf{H}^H\mathbf{H} + \lambda f^2\mathbf{I}_M\right)^{-1}\mathbf{H}^H}_{\tilde{\mathbf{P}}}\\
&\mathbf{P} = \frac{f}{\sqrt{\rho_f}}\underbrace{\left(\mathbf{H}^H\mathbf{H} + \lambda f^2\mathbf{I}_M\right)^{-1}\mathbf{H}^H}_{\tilde{\mathbf{P}}}\mathbf{N}^{-1}\\
&\mathbf{P} = \frac{f}{\sqrt{\rho_f}}\,\tilde{\mathbf{P}}\mathbf{N}^{-1}.
\end{aligned}
\tag{3-12}
$$

Using Wirtinger's calculus in (3-10) with respect to f yields:

$$
\begin{aligned}
\frac{\partial\mathcal{L}\left(\mathbf{P}, f, \lambda\right)}{\partial f} &= \sqrt{\rho_f}\mathrm{tr}\left(\mathbf{H}\mathbf{P}\mathbf{N}\mathbf{C}_s\right) + \sqrt{\rho_f}\mathrm{tr}\left(\mathbf{N}^H\mathbf{P}^H\mathbf{H}^H\mathbf{C}_s\right)\\
&\quad - 2f\rho_f\mathrm{tr}\left(\mathbf{N}^H\mathbf{P}^H\mathbf{H}^H\mathbf{H}\mathbf{P}\mathbf{N}\mathbf{C}_s\right) - 2f\mathrm{tr}\left(\mathbf{C}_w\right) = 0
\end{aligned}
\tag{3-13}
$$

$$
2\sqrt{\rho_f}\mathrm{Re}\left\{\mathrm{tr}(\mathbf{N}^H\mathbf{P}^H\mathbf{H}^H\mathbf{C}_s)\right\} = 2f\rho_f\mathrm{tr}(\mathbf{N}^H\mathbf{P}^H\mathbf{H}^H\mathbf{H}\mathbf{P}\mathbf{N}\mathbf{C}_s) + 2f\mathrm{tr}(\mathbf{C}_w)
\tag{3-14}
$$

Dividing the whole equation for 2 and f:

$$
\frac{\sqrt{\rho_f}}{f}\mathrm{Re}\left\{\mathrm{tr}(\mathbf{H}\mathbf{P}\mathbf{N}\mathbf{C}_s)\right\} = \rho_f\mathrm{tr}(\mathbf{N}^H\mathbf{P}^H\mathbf{H}^H\mathbf{H}\mathbf{P}\mathbf{N}\mathbf{C}_s) + \mathrm{tr}(\mathbf{C}_w)
\tag{3-15}
$$

Then using the result from (3-12):

$$
\begin{aligned}
&\mathrm{tr}\left(-\left(\rho_f\mathbf{N}^H\mathbf{P}^H\mathbf{H}^H\mathbf{H}\mathbf{P}\mathbf{N}\mathbf{C}_s + \mathbf{C}_w\right) = \frac{\sqrt{\rho_f}}{f}\,\mathrm{Re}\left(\mathbf{H}\mathbf{P}\mathbf{N}\mathbf{C}_s\right)\right)\\
&\mathrm{tr}\left(-\left(\rho_f\frac{f}{\sqrt{\rho_f}}\mathbf{N}^H\left(\mathbf{N}^{-1}\right)^H\tilde{\mathbf{P}}^H\mathbf{H}^H\mathbf{H}\frac{f}{\sqrt{\rho_f}}\,\tilde{\mathbf{P}}\mathbf{N}^{-1}\mathbf{N}\mathbf{C}_s + \mathbf{C}_w\right)\right.\\
&\qquad\left. = \frac{\sqrt{\rho_f}}{f}\,\mathrm{Re}\left(\mathbf{H}\frac{f}{\sqrt{\rho_f}}\,\tilde{\mathbf{P}}\mathbf{N}^{-1}\mathbf{N}\mathbf{C}_s\right)\right)\\
&\mathrm{tr}\left(-\left(f^2\tilde{\mathbf{P}}^H\mathbf{H}^H\mathbf{H}\,\tilde{\mathbf{P}}\mathbf{C}_s + \mathbf{C}_w\right) = \mathrm{Re}\left(\mathbf{H}\tilde{\mathbf{P}}\mathbf{C}_s\right)\right)\\
&\mathrm{tr}\left(\mathrm{Re}\left(\mathbf{H}\tilde{\mathbf{P}}\mathbf{C}_s\right)\right) = f^2\mathrm{tr}\left(\mathbf{H}^H\mathbf{H}\tilde{\mathbf{P}}\mathbf{C}_s\tilde{\mathbf{P}}^H\right) + \mathrm{tr}\left(\mathbf{C}_w\right)
\end{aligned}
\tag{3-16}
$$

Using the relation introduced in [41], we have

$$
\mathrm{tr}\left(\mathrm{Re}\left(\mathbf{H}\tilde{\mathbf{P}}\mathbf{C}_s\right)\right) = \mathrm{tr}\left(\left(\mathbf{H}^H\mathbf{H} + \epsilon\,\mathbf{I}_M\right)\tilde{\mathbf{P}}\mathbf{C}_s\tilde{\mathbf{P}}^H\right),
\tag{3-17}
$$

Equating (3-17) to (3-16), setting $\epsilon = \lambda f^2$ from (3-12) and using E_{tr}

restriction, it yields:

$$\begin{aligned}
&\mathrm{tr}\left(\left(\mathbf{H}^H\mathbf{H}+\epsilon\ \mathbf{I}_M\right)\tilde{\mathbf{P}}\mathbf{C}_s\tilde{\mathbf{P}}^H\right)=\mathrm{tr}\left(\mathbf{H}^H\mathbf{H}\tilde{\mathbf{P}}\mathbf{C}_s\tilde{\mathbf{P}}^H\right)+\frac{\mathrm{tr}\left(\mathbf{C}_w\right)}{f^2}\\
&\mathrm{tr}\left(\mathbf{H}^H\mathbf{H}\tilde{\mathbf{P}}\mathbf{C}_s\tilde{\mathbf{P}}^H\right)+\mathrm{tr}\left(\epsilon\tilde{\mathbf{P}}\mathbf{C}_s\tilde{\mathbf{P}}^H\right)=\mathrm{tr}\left(\mathbf{H}^H\mathbf{H}\tilde{\mathbf{P}}\mathbf{C}_s\tilde{\mathbf{P}}^H\right)+\frac{\mathrm{tr}\left(\mathbf{C}_w\right)}{f^2}\\
&f^2\mathrm{tr}\left(\epsilon\tilde{\mathbf{P}}\mathbf{C}_s\tilde{\mathbf{P}}^H\right)=\mathrm{tr}\left(\mathbf{C}_w\right)\\
&\epsilon f^2\mathrm{tr}\left(\tilde{\mathbf{P}}\mathbf{C}_s\tilde{\mathbf{P}}^H\right)=\mathrm{tr}\left(\mathbf{C}_w\right)\\
&\epsilon\mathrm{E}_{\mathrm{tr}}=\mathrm{tr}\left(\mathbf{C}_w\right)\\
&\epsilon=\frac{\mathrm{tr}\left(\mathbf{C}_w\right)}{\mathrm{E}_{\mathrm{tr}}}
\end{aligned}\tag{3-18}$$

since

$$\begin{aligned}
\mathrm{E}_{\mathrm{tr}}&=\rho_f\mathrm{tr}\left(\mathbf{P}\mathbf{N}\mathbf{C}_s\mathbf{N}^H\mathbf{P}^H\right)\\
&=\rho_f\mathrm{tr}\left(\frac{f}{\sqrt{\rho_f}}\ \tilde{\mathbf{P}}\mathbf{N}^{-1}\mathbf{N}\mathbf{C}_s\mathbf{N}^H\left(\mathbf{N}^{-1}\right)^H\tilde{\mathbf{P}}^H\frac{f}{\sqrt{\rho_f}}\right)\\
&=f^2\mathrm{tr}\left(\tilde{\mathbf{P}}\mathbf{C}_s\tilde{\mathbf{P}}^H\right).
\end{aligned}\tag{3-19}$$

With the result above, we arrive at:

$$f_{\mathrm{MMSE}}=\sqrt{\frac{\mathrm{E}_{\mathrm{tr}}}{\mathrm{tr}\left(\tilde{\mathbf{P}}\mathbf{C}_s\tilde{\mathbf{P}}^H\right)}},\tag{3-20}$$

Finally, the MMSE precoder that takes into account power allocation for cell-free and multi-cell systems is written as:

$$\mathbf{P}_{\mathrm{MMSE}}=\frac{f_{\mathrm{MMSE}}}{\sqrt{\rho_f}}\left(\mathbf{H}^H\mathbf{H}+\frac{\mathrm{tr}\left(\mathbf{C}_w\right)}{\mathrm{E}_{\mathrm{tr}}}\mathbf{I}_M\right)^{-1}\mathbf{H}^H\mathbf{N}^{-1},\tag{3-21}$$

As mentioned before, $\mathbf{H}$, $\mathbf{N}$ and $\mathbf{C}_w$ dimensions are different for each system, so $\mathbf{P}_{\mathrm{MMSE,\ CF}}\in\mathbb{C}^{M\times K}$ and $\mathbf{P}_{\mathrm{MMMSE,\ MC}}\in\mathbb{C}^{N_t\times N_r}$.

3.2 Power Allocation

In this section, we will describe the achievable rates for the MMSE precoder and different power allocation techniques (UPA, APA and R-APA) to maximize SINR aiming to achieve excellent bits / Hz / channel use rates. As demonstrated in Chapter 2, the system capacity is subjected to the power constraint E_{tr}, which depends on $\mathbf{P}$ and $\mathbf{N}$ as show in (3-19).

Subsection 2.3 has shown that system rates depend on decent power coefficient allocation η_{mi} used by antenna m to transmit to user i for SINR calculation. For that reason, we first use the UPA technique presented in [15]

and [16], next we develop APA and R-APA techniques to calculate $\mathbf{N}$, a diagonal matrix with $\sqrt{\eta_1}, \ldots, \sqrt{\eta_K}$ on its main diagonal, which is used to recompute the precoder $\mathbf{P}_{\text{MMSE}}$ and find the power allocation matrix $\mathbf{N}_{\text{MMSE}}$. The MMSE achievable sum-rate of all users, assuming Gaussian signalling:

$$R_{\text{MMSE}} = \sum_{k=1}^{K} \log_2(1 + \text{SINR}_{k,\text{MMSE}}), \tag{3-22}$$

where

$$\text{SINR}_{k,\text{MMSE}} = \frac{\mathbb{E}\left[|A_1|^2\right]}{\sigma_w^2 + \sum_{i=1, i\neq k}^{K} \mathbb{E}\left[|A_{2,i}|^2\right] + \mathbb{E}\left[|A_3|^2\right]}. \tag{3-23}$$

A_1 is the term that contains the desired signal, $A_{2,i}$ is the interference caused by user i and A_3 is the residual interference originated from the imperfect CSIT. Considering system equation in (2-35) and (3-21), we expand the terms to obtain the received signal by user k:

$$\begin{aligned} y_k &= \sqrt{\rho_f}\ \mathbf{h}_k \mathbf{P}_{\text{MMSE}}\ \mathbf{N}_{\text{MMSE}}\ \mathbf{s} + w_k \\ &= \sqrt{\rho_f}\ \left(\mathbf{h}_k + \tilde{\mathbf{h}}_k\right) \frac{f_{\text{MMSE}}}{\sqrt{\rho_f}} \left(\mathbf{H}^H\mathbf{H} + \frac{K\sigma_w^2}{\text{E}_{\text{tr}}}\mathbf{I}_M\right)^{-1} \mathbf{H}^H\mathbf{N}^{-1}\mathbf{N}_{\text{MMSE}}\ \mathbf{s} + w_k \\ &= \underbrace{\sqrt{\rho_f}\ \mathbf{h}_k \frac{f_{\text{MMSE}}}{\sqrt{\rho_f}} \left(\mathbf{H}^H\mathbf{H} + \frac{K\sigma_w^2}{\text{E}_{\text{tr}}}\mathbf{I}_M\right)^{-1} \mathbf{H}^H\mathbf{N}^{-1}\mathbf{N}_{\text{MMSE}}\ \mathbf{s} +}_{\text{desired signal + interference}} \\ &\quad \underbrace{\sqrt{\rho_f}\ \tilde{\mathbf{h}}_k \frac{f_{\text{MMSE}}}{\sqrt{\rho_f}} \left(\mathbf{H}^H\mathbf{H}^H + \frac{K\sigma_w^2}{\text{E}_{\text{tr}}}\mathbf{I}_M\right)^{-1} \mathbf{H}^H\mathbf{N}^{-1}\mathbf{N}_{\text{MMSE}}\ \mathbf{s} + w_k,}_{\text{CSI error}} \end{aligned} \tag{3-24}$$

where $\mathbf{h}_k = [h_{1,k}, \ldots, h_{M,k}]$ is the CSI vector for user k and $\tilde{\mathbf{h}}_k = [\tilde{h}_{1,k}, \ldots, \tilde{h}_{M,k}]$ is the CSI error vector for user k.

We arrive at the values to input in (3-23):

$$A_1 = \sqrt{\rho_f}\mathbf{h}_k\mathbf{p}_k\sqrt{\eta_k}s_k, \tag{3-25}$$

is the desired signal,

$$A_{2,i} = \sqrt{\rho_f}\mathbf{h}_k\mathbf{p}_i\sqrt{\eta_i}s_i, \text{ for } i \neq k,\ i = 1, \ldots, K, \tag{3-26}$$

is the interference caused by user i in user k and

$$A_3 = \sqrt{\rho_f}\tilde{\mathbf{h}}_k\mathbf{P}_{\text{MMSE}}\mathbf{N}_{\text{MMSE}}\mathbf{s} \tag{3-27}$$

refers to CSI error.

In order to allocate power to the system, we need to derive the per antenna power constraint, therefore the transmitted power for the mth antenna

can be expressed as:

$$\begin{aligned}\rho_f \mathbb{E}\left[\mathbf{a}_m^T \mathbf{a}_m^*\right] &= \rho_f \mathbb{E}\left[\mathbf{N}_{\text{MMSE}} \mathbf{p}_m^T \mathbf{p}_m^* \mathbf{N}_{\text{MMSE}}\right] \\ &= \rho_f \text{tr}\left(\mathbb{E}\left[\mathbf{N}_{\text{MMSE}} \mathbf{p}_m^T \mathbf{p}_m^* \mathbf{N}_{\text{MMSE}}\right]\right) \\ &= \rho_f \text{tr}\left(\mathbf{N}_{\text{MMSE}}^2 \mathbb{E}\left[\mathbf{p}_m^T \mathbf{p}_m^*\right]\right) \\ &= \rho_f \sum_{i=1}^{K} \eta_i \delta_{m,i}\end{aligned} \tag{3-28}$$

where

$$\boldsymbol{\delta}_m = \text{diag}\left\{\mathbb{E}\left[\mathbf{p}_m^T \mathbf{p}_m^*\right]\right\}, m = 1, \ldots, M, \tag{3-29}$$

$\mathbf{a}_m$ is the mth row of matrix $\mathbf{A} = \mathbf{P}_{\text{MMSE}} \mathbf{N}_{\text{MMSE}}$, $\mathbf{p}_m = [p_{m,1}, \ldots, p_{m,K}]$ is the mth row of the precoder $\mathbf{P}_{\text{MMSE}}$ and $\delta_{m,i}$ is the ith element of vector $\boldsymbol{\delta}_m$. The maximum transmitted power per-antenna is ρ_f, resulting in the following per-antenna power constraint

$$\begin{aligned}\rho_f \sum_{i=1}^{K} \eta_i \delta_{m,i} \leq \rho_f, m = 1, \ldots, M, \\ \sum_{i=1}^{K} \eta_i \delta_{m,i} \leq 1, m = 1, \ldots, M.\end{aligned} \tag{3-30}$$

Therefore, the max-min fairness power allocation problem with antenna power constraint becomes

$$\max_{\boldsymbol{\eta}} \min_{k} \text{SINR}_k(\boldsymbol{\eta}) \tag{3-31a}$$

$$\text{s.t.} \sum_{i=1}^{K} \eta_i \delta_{m,i} \leq 1, m = 1, \ldots, M, \tag{3-31b}$$

In systems equations 2-35, we consider the matrix $\mathbf{N}$ as $\mathbf{N}_{mc} \in \mathbb{C}^{N_r \times N_r}$ and $\mathbf{N}_{cf} \in \mathbb{C}^{K \times K}$. However, in both cases we can consider the matrix presented in (2-28), with k as the number of receive antennas.

In the following subsections, we will present in details power allocation techniques to adjust the power coefficients $\boldsymbol{\eta}$ in MMSE design approach for the best $\mathbf{N}$ allocation.

3.2.1 Uniform Power Allocation (UPA)

We would like to find the power coefficient, η that maximize the minimum SINR_k. As a first approach of power allocation technique, UPA considers perfect channel estimation, meaning CSI error is zero, and takes into account a per-antenna power constraint. Basically, we find the antenna m or N_t that

transmit in full-power and equal values for η_k. The minimum possible value for η_k is:

$$\eta_k = 1/\left(\max_m \sum_{i=1}^{K} \delta_{m,i}\right),\ k = 1, \ldots, K, \tag{3-32}$$

where $\delta_{m,i}$ is the ith element of vector $\boldsymbol{\delta}_m$.

We can mention that UPA has very low computational complexity when compared to Optimal Power Allocation (OPA) presented in [15] and [16], where the optimization problem is taken to Matlab Software for Discipline Convex Programming (CVX).

3.2.2 Adaptive Power Allocation (APA)

APA initiative aims to adjust the power coefficients η_k so that they minimize the effect of the interference at the received signal vector $\mathbf{y}$ [42, 43]. We propose that the matrix $\mathbf{N}$ start with a set of defined η. We consider the MSE cost function in (3-6) to calculate the instantaneous gradient, using Wirting's calculus with respect to $\mathbf{N}^*$:

$$\begin{gathered}\nabla\mathbf{C}(\mathbf{N}) = \frac{\partial\mathbf{C}(\mathbf{N})}{\partial\mathbf{N}^*} \\ \nabla\mathbf{C}(\mathbf{N}) = -f\sqrt{\rho_f}\mathbf{P}^H\mathbf{H}^H\mathbf{C}\mathbf{s} + f^2\rho_f\mathbf{P}^H\mathbf{H}^H\mathbf{H}\mathbf{P}\mathbf{N}\mathbf{C}\mathbf{s}\end{gathered} \tag{3-33}$$

We use the result of this derivation to find the matrix $\mathbf{N}$ from the update below, where μ is the step size of the APA algorithm:

$$\mathbf{N}[i+1] = \mathbf{N}[i] - \mu\nabla\mathbf{C}(\mathbf{N}) \tag{3-34}$$

Then, we apply per-antenna power constraint in order to fulfil power requirement. Finally, we obtain the final value for $\mathbf{N}$.

The Algorithm 1 is the adaptive SG learning strategy that performs APA, explained in details:

Algorithm 1 APA Algorithm Based on the Stochastic Gradient

Parameters: μ (step size) and T_{APA} (number of iterations).
Initialization: $\eta_k[0] = 10^{-3}, k = 1, \ldots, K$.
For i= 0:T_{APA}
  Set $\mathbf{N}[i]$ as a diagonal matrix with $\sqrt{\boldsymbol{\eta}[i]}$ on its diagonal.
  Define $\mathcal{C}(\mathbf{N})$.
  Compute $\nabla C(N)$.
  Calculate $\mathbf{N}[i+1] = \mathbf{N}[i] - \mu \hat{\nabla}_{\mathbf{N}^*} \mathcal{C}(\mathbf{N})$
  Obtain $\eta[i+1] = \mathbf{N}[i+1] \odot \mathbf{I}_K$
  Apply the per-antenna constraint $\boldsymbol{\delta}_m \cdot \boldsymbol{\eta}[i+1] \leq 1, m = 1, \ldots, M$ to adjust $\mathbf{N}[i+1]$
end
Obtain $\mathbf{N} = \mathbf{N}[i+1]$.

3.2.3 Robust Adaptive Power Allocation (R-APA)

The principles for the R-APA approach are the same as APA, namely, to use an SG algorithm to recalculate $\mathbf{N}$ as demostrated in Algorithm 1). However, we consider imperfect CSIT on the MSE cost function, in order to ensure better performance and practical estimation.

In this case, the channel assumes value $\mathbf{H} = \hat{\mathbf{H}} + \tilde{\mathbf{H}}$, where the matrix $\hat{\mathbf{H}}$ represents the channel estimate and the matrix $\tilde{\mathbf{H}}$ models the CSIT imperfection by adding the error of the estimation procedure. $\mathbf{H} \in N_r \times N_t$ in MC and $\in M \times K$ in CF. Each coefficient h_{ij} of the matrix $\mathbf{H}$ represents the link between the i-th receive antenna and the j-th transmit antenna. The channel matrix can be expressed by $\mathbf{H} = [\mathbf{H}_1, \mathbf{H}_2, \ldots, \mathbf{H}_K]$, where $\mathbf{H}_K$ denotes the channel connecting the BS/AP to the k-th user.

Let us now reconsider the MSE function (3-6) and rewrite it with the new definition of $\mathbf{H}$:

$$\mathbf{C}(\mathbf{N_{rob}}) = \mathbb{E}\{|\mathbf{s} - \hat{\mathbf{H}}\mathbf{P}\mathbf{N}\mathbf{s} - \tilde{\mathbf{H}}\mathbf{P}\mathbf{N}\mathbf{s} - \mathbf{n}|_2^2\} \tag{3-35}$$

Let us expand the terms to find $\mathbf{C}(\mathbf{N_{robust}})$:

$$\begin{aligned}\mathbf{C}(\mathbf{N_{rob}}) = \mathbb{E}[&(\mathbf{s}^H\mathbf{s}) - (\mathbf{s}^H\tilde{\mathbf{H}}\mathbf{P}\mathbf{N}\mathbf{s}) - (\mathbf{s}^H\hat{\mathbf{H}}\mathbf{P}\mathbf{N}\mathbf{s}) - (\mathbf{s}^H\mathbf{n}) \\ &-(\mathbf{s}^H\mathbf{N}^H\mathbf{P}^H\hat{\mathbf{H}}^H\mathbf{s}) + (\mathbf{s}^H\mathbf{N}^H\mathbf{P}^H\hat{\mathbf{H}}^H\hat{\mathbf{H}}\mathbf{P}\mathbf{N}\mathbf{s}) \\ &+(\mathbf{s}^H\mathbf{N}^{\mathbf{HP}H}\hat{\mathbf{H}}^H\tilde{\mathbf{H}}\mathbf{P}\mathbf{N}\mathbf{s}) + (\mathbf{s}^H\mathbf{N}^H\mathbf{P}^H\hat{\mathbf{H}}^H\mathbf{n}) \\ &-(\mathbf{s}^H\mathbf{N}^H\mathbf{P}^H\tilde{\mathbf{H}}^H\mathbf{s}) + (\mathbf{s}^H\mathbf{N}^H\mathbf{P}^H\tilde{\mathbf{H}}^H\hat{\mathbf{H}}\mathbf{P}\mathbf{N}\mathbf{s}) \\ &+(\mathbf{s}^H\mathbf{N}^H\mathbf{P}^H\tilde{\mathbf{H}}^H\tilde{\mathbf{H}}\mathbf{P}\mathbf{N}\mathbf{s}) + (\mathbf{s}^H\mathbf{N}^H\mathbf{P}^H\tilde{\mathbf{H}}^H\mathbf{n}) \\ &-(\mathbf{n}^H\mathbf{s}) + (\mathbf{n}^H\hat{\mathbf{H}}\mathbf{P}\mathbf{N}\mathbf{s}) + (\mathbf{n}^H\tilde{\mathbf{H}}\mathbf{P}\mathbf{N}\mathbf{s}) + (\mathbf{n}^H\mathbf{n})]\end{aligned} \tag{3-36}$$

where $\mathbf{x}$ and $\mathbf{n}$ are statistically independent, as well as $\tilde{\mathbf{H}}$ and $\hat{\mathbf{H}}$. Applying the trace operator, we have:

$$\begin{gathered}\mathbf{C}(\mathbf{N_{rob}}) = \mathrm{tr}(\mathbf{C_s}) - 2\mathrm{tr}(\hat{\mathbf{H}}\mathbf{P}\mathbf{N}\mathbf{C_s}) \\ +2\mathrm{tr}(\mathbf{N}^H\mathbf{P}^H\hat{\mathbf{H}}^H\hat{\mathbf{H}}\mathbf{P}\mathbf{N}\mathbf{C_s}) + \mathrm{tr}(\mathbf{N}^H\mathbf{P}^H\tilde{\mathbf{H}}^H\tilde{\mathbf{H}}\mathbf{P}\mathbf{N}\mathbf{C_s}) \\ +\mathrm{tr}(\mathbf{C_n})\end{gathered} \tag{3-37}$$

Assuming that the vectors $\tilde{\mathbf{h}}_k$ and $\tilde{\mathbf{h}}_j$ are independent, i.e., $E\left[\tilde{\mathbf{h}}_k^H\tilde{\mathbf{h}}_j\right] = 0$ with $(k \neq j)$ and $E\left[\tilde{\mathbf{h}}_k^H\tilde{\mathbf{h}}_k\right] = \sigma_{e_k}^2$, we obtain:

$$E[\tilde{\mathbf{H}}^H\tilde{\mathbf{H}}] = [\tilde{\mathbf{G}}] = \begin{bmatrix}\sigma_{e_1}^2 & 0 & \dots & 0 \\ 0 & \sigma_{e_2}^2 & \dots & 0 \\ \vdots & \vdots & \ddots & \vdots \\ 0 & 0 & \dots & \sigma_{e_{N_t}}^2\end{bmatrix} \tag{3-38}$$

Without loss of generality, we consider $\sigma_{e_i}^2 = \sigma_{e_j}^2$, furthermore $\sigma_{e_i}^2 = N_r\sigma_e^2$

$$[\tilde{\mathbf{G}}] = N_r\begin{bmatrix}\sigma_e^2 & 0 & \dots & 0 \\ 0 & \sigma_e^2 & \dots & 0 \\ \vdots & \vdots & \ddots & \vdots \\ 0 & 0 & \dots & \sigma_e^2\end{bmatrix} \tag{3-39}$$

We then compute $\nabla\mathbf{C}(\mathbf{N_{rob}})$:

$$\begin{gathered}\nabla\mathbf{C}(\mathbf{N_{rob}}) = \frac{\partial\mathbf{C}(\mathbf{N_{rob}})}{\partial\mathbf{N}} \\ \nabla\mathbf{C}(\mathbf{N_{rob}}) = -2(\hat{\mathbf{H}}\mathbf{P}\mathbf{C_s}) + 2(\mathbf{P}^H\hat{\mathbf{H}}^H\hat{\mathbf{H}}\mathbf{P}\mathbf{N}\mathbf{C_s}) \\ +(\mathbf{P}^H[\tilde{\mathbf{G}}]\mathbf{P}\mathbf{N}\mathbf{C_s})\end{gathered} \tag{3-40}$$

The result from (3-40) can be used to update the matrix $\mathbf{N}$ by the gradient descent recursion:

$$\mathbf{N}[i+1] = \mathbf{N}[i] - \mu\nabla\mathbf{C}(\mathbf{N_{rob}}) \tag{3-41}$$

Including imperfect CSIT to the recursion of power allocation coefficients, increases robustness against CSIT uncertainties.

3.2.3.1 Computational Complexity of R-APA

In this subsection, we demonstrate the computational complexity calculation for the R-APA approach [44], considering $\hat{\mathbf{H}}$ as estimated channel matrix and $\tilde{\mathbf{H}}$ as CSIT imperfections, where both $\in \mathbb{C}^{M\times K}$, $\mathbf{P} \in \mathbb{C}^{M\times K}$, $\mathbf{N} \in \mathbb{C}^{K\times K}$, then $\mathbf{C}_s \in \mathbb{R}^{K\times K}$. We use the expression in (3-41):

$$\begin{aligned}\mathbf{N}[i+1] = \mathbf{N}[i] - \mu(-2(\hat{\mathbf{H}}\mathbf{P}\mathbf{C_s}) + 2(\mathbf{P}^H\hat{\mathbf{H}}^H\hat{\mathbf{H}}\mathbf{P}\mathbf{N}\mathbf{C_s}) \\ + \mathbf{P}^H[\tilde{\mathbf{G}}]\mathbf{P}\mathbf{N}\mathbf{C_s})\end{aligned} \tag{3-42}$$

where $[\tilde{\mathbf{G}}] = E[\tilde{\mathbf{H}}^H\tilde{\mathbf{H}}]$.

$\hat{\mathbf{H}}\mathbf{P} \rightarrow MK^2$ multiplications $+ K^2(M-1)$ additions.
$\hat{\mathbf{H}}\mathbf{P}\mathbf{C_s} \rightarrow K^3$ multiplications $+ K^2(K-1)$ additions.
$2(\hat{\mathbf{H}}\mathbf{P}\mathbf{C_s}) \rightarrow K^2$ multiplications.
$\mathbf{P}^H\hat{\mathbf{H}}^H \rightarrow MK^2$ multiplications $+ K(M-1)$ additions.
$\mathbf{P}^H\hat{\mathbf{H}}^H\hat{\mathbf{H}} \rightarrow MK^2$ multiplications $+ MK(K-1)$ additions.
$\mathbf{P}^H\hat{\mathbf{H}}^H\hat{\mathbf{H}}\mathbf{P} \rightarrow MK^2$ multiplication $+ K^2(M-1)$ additions.
$\mathbf{P}^H\hat{\mathbf{H}}^H\hat{\mathbf{H}}\mathbf{P}\mathbf{N}[i] \rightarrow K^3$ multiplication $+ K^2(K-1)$ additions.
$\mathbf{P}^H\hat{\mathbf{H}}^H\hat{\mathbf{H}}\mathbf{P}\mathbf{N}[i]\mathbf{C_s} \rightarrow K^3$ multiplication $+ K^2(K-1)$ additions.
$2(\mathbf{P}^H\hat{\mathbf{H}}^H\hat{\mathbf{H}}\mathbf{P}\mathbf{N}[i]\mathbf{C_s}) \rightarrow K^2$ multiplication
$\mathbf{P}^H\tilde{\mathbf{H}}^H\tilde{\mathbf{H}} \rightarrow MK^2$ multiplications $+ MK(K-1)$ additions.
$\mathbf{P}^H\tilde{\mathbf{H}}^H\tilde{\mathbf{H}}\mathbf{P} \rightarrow MK^2$ multiplications $+ K^2(M-1)$ additions.
$\mathbf{P}^H\tilde{\mathbf{H}}^H\tilde{\mathbf{H}}\mathbf{P}\mathbf{N}[i] \rightarrow K^3$ multiplications $+ K^2(K-1)$ additions.
$\mathbf{P}^H\tilde{\mathbf{H}}^H\tilde{\mathbf{H}}\mathbf{P}\mathbf{N}[i]\mathbf{C_s} \rightarrow K^3$ multiplications $+ K^2(K-1)$ additions.
$-2(\hat{\mathbf{H}}\mathbf{P}\mathbf{C_s}) + 2(\mathbf{P}^H\hat{\mathbf{H}}^H\hat{\mathbf{H}}\mathbf{P}\mathbf{N}\mathbf{C_s}) + \mathbf{P}^H[\tilde{\mathbf{G}}]\mathbf{P}\mathbf{N}\mathbf{C_s}$
$\rightarrow K^3$ additions.
$\mathbf{N}[i] - \mu(-2(\hat{\mathbf{H}}\mathbf{P}\mathbf{C_s}) + 2(\mathbf{P}^H\hat{\mathbf{H}}^H\hat{\mathbf{H}}\mathbf{P}\mathbf{N}\mathbf{C_s}) + \mathbf{P}^H[\tilde{\mathbf{G}}]\mathbf{P}\mathbf{N}\mathbf{C_s})$
$\rightarrow K^2$ multiplications $+ K^2$ additions.

(3-43)

Overall Complexity:

$$\begin{aligned}\text{Multiplications } &= T_{\text{R-APA}}\Big(MK^2 + K^3 + K^2 + MK^2 + MK^2 + MK^2 + K^3 \\ &+ K^3 + K^2 + MK^2 + MK^2 + K^3 + K^3 + K^3 + K^2 \\ &= T_{\text{R-APA}}\Big(6MK^2 + 6K^3 + 3K^2\Big) \\ \text{Additions } &= T_{\text{APA}}\Big(K^2(M-1) + K^2(K-1) + K(M-1) + MK(K-1) \\ &+ K^2(M-1) + K^2(K-1) + K^2(K-1) + MK(K-1) + K^2(M-1) \\ &+ K^2(K-1) + K^2(M-1) + K^3 + K^2) \\ &= T_{\text{R-APA}}\Big(M\Big(5K^2 - K\Big) - 2K^2 + K^3 - K\Big)\end{aligned} \tag{3-44}$$

According to the Big O notation, the complexity of the R-APA algorithm

is $\mathcal{O}\left(T_{\text{R-APA}}MK^2\right)$ and APA is $\mathcal{O}\left(T_{\text{APA}}MK^2\right)$

3.3 Computational Complexity of Analyzed Techniques

During this work, some MIMO techniques were described in its mathematical model and, then, transformed into an algorithm. Well designed algorithms allow optimized rates, performance and expenses for the systems. The computational complexity intends to measure the amount of resources (normally time and memory) required to run the algorithm.

In Table 3.1 we summarize the computational complexity for each technique covered in this work: Precoding, SINR calculation and power allocation. The calculation of the results presented are in Appendix A.

Table 3.1: Computational Complexity

Precoding	MMSE Precoder	$\mathcal{O}\left(M^3\right)$
	ZF Precoder	$\mathcal{O}\left(M^3\right)$
	CB Precoder	$\mathcal{O}\left(MK\right)$
SINR Computation	MMSE Precoder	$\mathcal{O}\left(M^2K^2\right)$
	ZF Precoder	$\mathcal{O}\left(M^2K^2\right)$
	CB Precoder	$\mathcal{O}\left(MK^2\right)$
Power Allocation	OPA	$\mathcal{O}\left(T_{\text{OPA}}K^{3.5}\right)$
	R-APA	$\mathcal{O}\left(T_{\text{R-APA}}MK^2\right)$
	APA	$\mathcal{O}\left(T_{\text{APA}}MK^2\right)$
	UPA	$\mathcal{O}\left(MK^2\right)$

Starting with the precoders, the complexity of the MMSE precoder is comparable to the ZF precoder from [15]. The CB precoder, [13, 15], however, presents much lower computational complexity, at the cost of degraded performance. The same can be said in terms of SINR computation. When power allocation techniques are analyzed, the result depends on the number of iterations of the bisection method, $T_{\text{OPA}}, T_{\text{R-APA}}$ and T_{APA}. If they are all the same, OPA method will be the most costly. Another observation, R-APA and APA [16, 19] normally requires less iterations than OPA, proving its much lower complexity. UPA is proven to be the least complex of all, however in terms of performance is not the best. If $M^2K^2 > T_{\text{R-APA}}MK^2$, the computational cost of MMSE + R-APA will be $\mathcal{O}\left(M^2K^2\right)$. We conclude that the

proposed R-APA has very reasonable computational cost and can outperform existing techniques.

3.4 Numerical Results

In this section, we study the performance of both systems architectures in terms of BER vs. SNR and sum-rate vs. SNR. Three linear precoding techniques, Matched-Filter (MF) or Conjugated Beamforming (CB), Zero-Forcing (ZF) and Minimum Mean Squared Error (MMSE), were used for simulation purposes. We also compare Uniform Power Allocation (UPA) and Adaptive Power Allocation (APA) with the robust R-APA technique proposed in this work.

We combined different systems architectures, precoding and power allocation techniques. When describing an approach we will use the following notation:

– Architecture + Precoding + Power Allocation

For each category, we have the following models:

– Architecture: CF and MC;
– Precoding: CB, ZF and MMSE;
– Power Allocation: R-APA, APA and UPA.

First of all, we reviewed MIMO transmission in Section 2.5, increasing the number of Tx and Rx antennas in Fig. 2.12. In this new setup, K=8 and M=16, initially with only one cell, adding MMSE precoder explained in this chapter. For math simplicity, the simulation was performed using QPSK modulation, UPA technique, 1000 packets transmitted and considered Rayleight fading channel. When the three linear precoder studied in this work are compared, we clearly see a much better performance in MMSE and ZF designs, where in very low SNR rates accomplished no more bit errors (achieved 0 BER at 5 dB). We can also highlight that CB stays constant close to 10^{-3}. In all three schemes, the results are excellent, with rates very close to 0 for very low SNR.

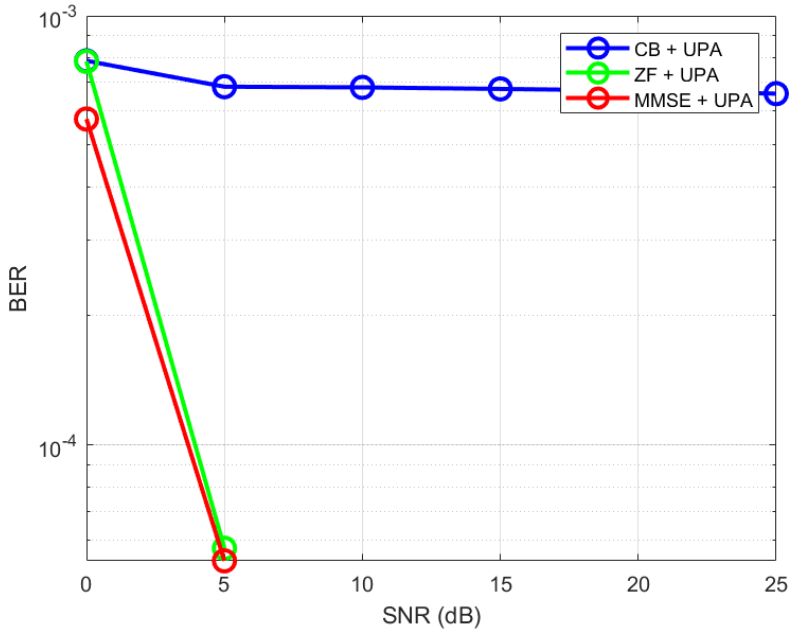

Figure 3.1: System Performance: One-Cell with K = 8 and M = 16.

To expand the discussion and study MC properties, we used the same parameters for the algorithms as the simulation above, and introduced more cells to the system with a 4 cells cluster. We can clearly see how inter-cell interference and user interference decrease system performance. In Fig. 3.2, we see the performance of ZF and MMSE precoder have near BER × SNR evolution, close to 10^{-1} at 20 dB in this use case. CB outperforms both precoders until approximately 3 dB, when the other two precoders surpassed it and achieved better rates until the end of the simulation.

Furthermore, we examined MC systems capacity in terms of Sum Rate × SNR. In Fig. 3.3, we observed that MC + CB had a constant capacity of 5 bit/Hz/s when we increased the SNR. The performance of MC + MMSE and MC + ZF were close to 20 bit/Hz/s constantly after 15 dB. At low SNR values, MC + MMSE had more 5 bit/Hz/s than MC + ZF, in terms of system capacity.

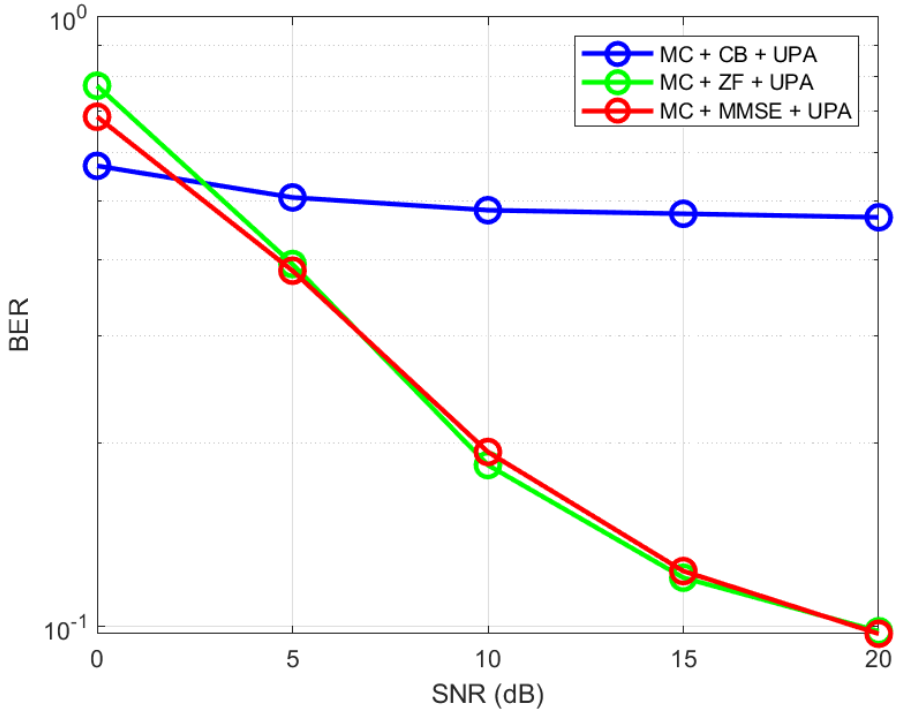

Figure 3.2: System Performance: Multi-Cell with C=4, K = 4 and M = 8.

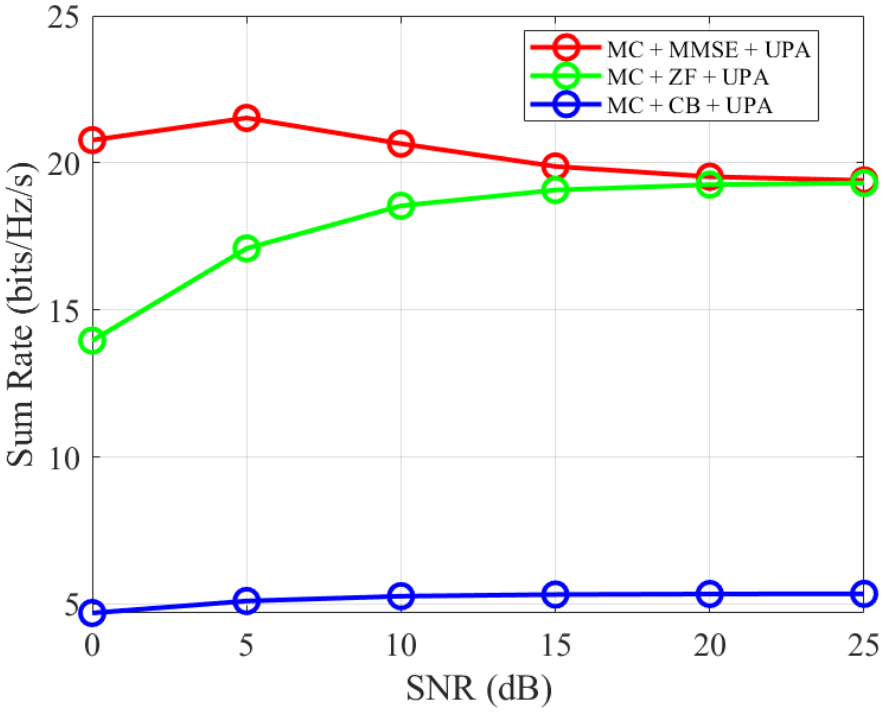

Figure 3.3: System Sum-rate: Multi-Cell with C=4, K = 4 and M = 8.

In the next experiment, we have CF initial analysis, allowing our first comparison to MC. We considered the same mathematical structure and parameter as previous simulation, with QPSK modulation and fading discussed

in the literature review. For complete equality between systems, we make the discussion over an area of coverage with equal number of users and antennas, such as:

$$\begin{aligned} K_{CF} &= CK_{MC} \\ M_{CF} &= CM_{MC} \end{aligned} \tag{3-45}$$

We notice that the results from Fig. 3.2 and Fig. 3.4 are close to each other (around 10^{-1}). However, we see a better performance in CF overall, where MMSE achieved less than 10^{-1} after 15 dB. We are using the UPA technique in both cases, for that reason we will not take power allocation into consideration in this investigation. As mentioned, at very low rates of SNR, in MC + CB the results are the best until 3dB, then MC + ZF and MC + MMSE outperforms it with very close conducting among the two. In CF systems, CF + MMSE clearly had better BER presentation. CF + ZF and CF + CB had very similar development. In both study cases, MMSE precoder have a very good performance in general, outperforming CF + ZF, CF + CB and MC + CB.

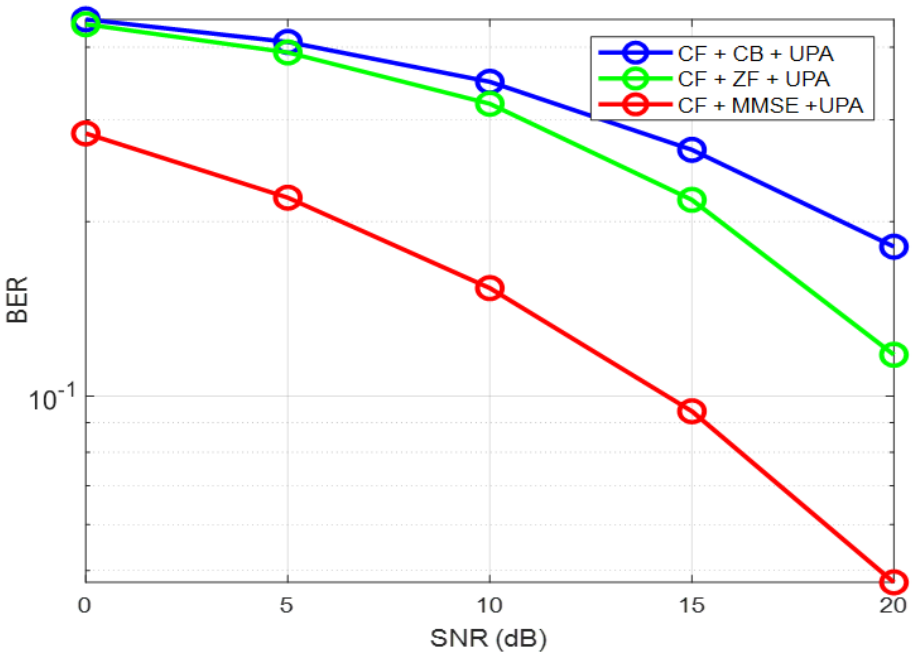

Figure 3.4: System Performance: Cell-Free with K = 16 and M = 32.

We now introduce the power allocation method R-APA developed in this work and compared its performance to UPA (demonstrated above) and APA techniques. We also increased the number of transmitting antennas of

the system, and maintained the number of receiving antennas. In Fig. 3.5, we noticed that MMSE linear precoder design was the one with best rate among CB and ZF, as studied before. Adding to that, the iterative APA approach brings a good enhancement of performance over UPA adjusting matrix **N**. Using CSIT imperfection in its system model derivation with R-APA, we can get even a better improvement after 5 dB. For high SNR values, CF + MMSE + R-APA progress were even better.

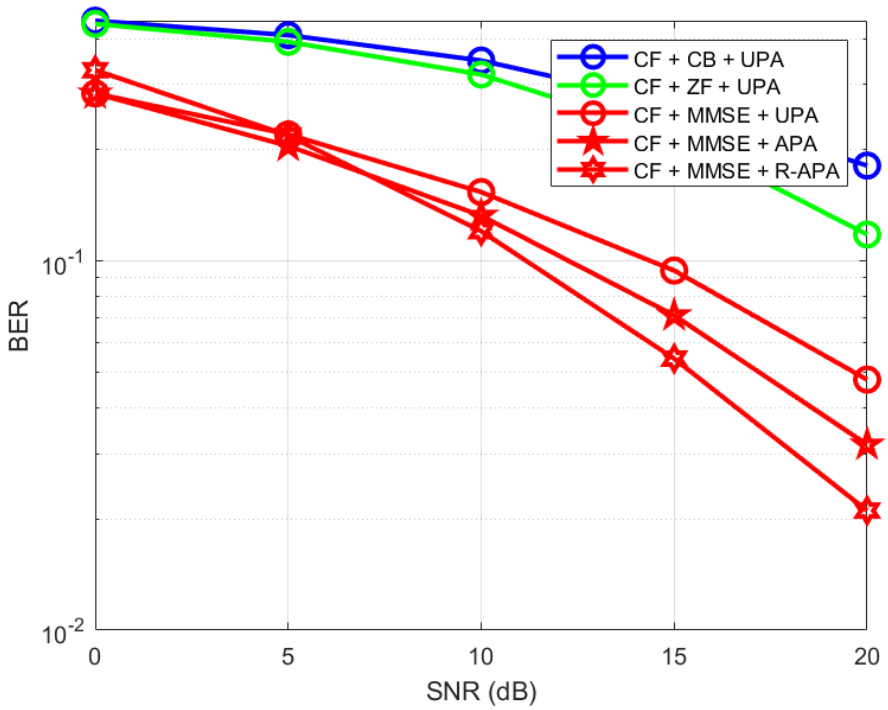

Figure 3.5: System Performance: Cell-Free with K = 16 and M = 64.

Next, in Fig. 3.6 we observed the Sum-Rate × SNR in CF System with three linear precoder and three different power allocation techniques. We noted an increase in the system capacity due to the increment in the number of Tx antennas. The MMSE precoder had better capacity than CF + CB + UPA and CF + ZF + UPA since the beginning of the simulation, starting at 10 bits/Hz/s. The simulations for R-APA and APA algorithm used μ=0.25 and 5 iterations. When comparing power allocation techniques in the MMSE precoder, APA and R-APA approaches constantly increased the outcome when compared to to UPA for the whole simulation (from 0 to 25 dB).

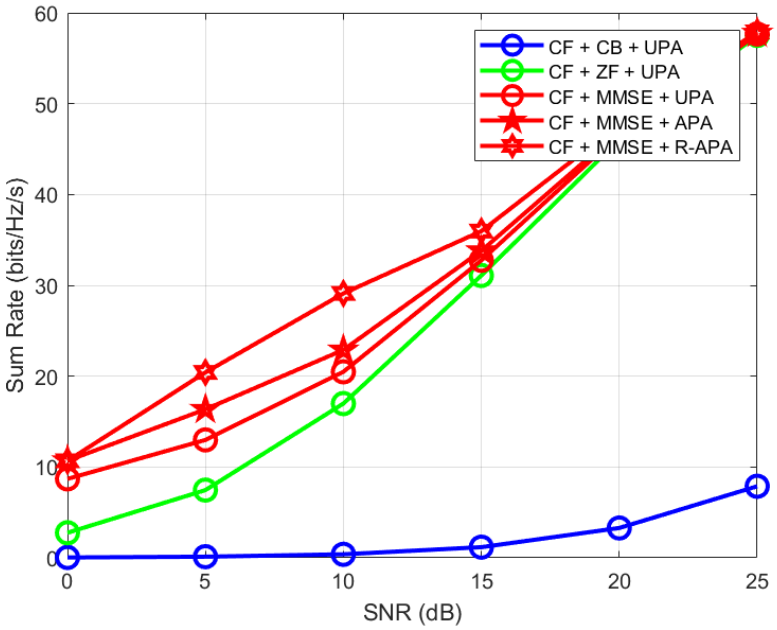

Figure 3.6: System Sum-rate: Cell-Free with K = 16 and M = 64.

Then, we observed the results of the MC architecture when we applied R-APA and APA techniques. First of all, the increment in the number of transmitting antennas in each cell, boosted the performance of MC + ZF + UPA and MC + MMSE + UPA when compared to Fig. 3.2. They both arrived at 10^{-1} at 10 SNR. In Fig. 3.7, we explored the three types of linear precoders and three power allocation techniques, similarly to previous analysis. We can see that MMSE outperforms ZF and MF (which is almost constant) using UPA. Furthermore, MMSE using APA and R-APA have better results than MMSE + UPA.

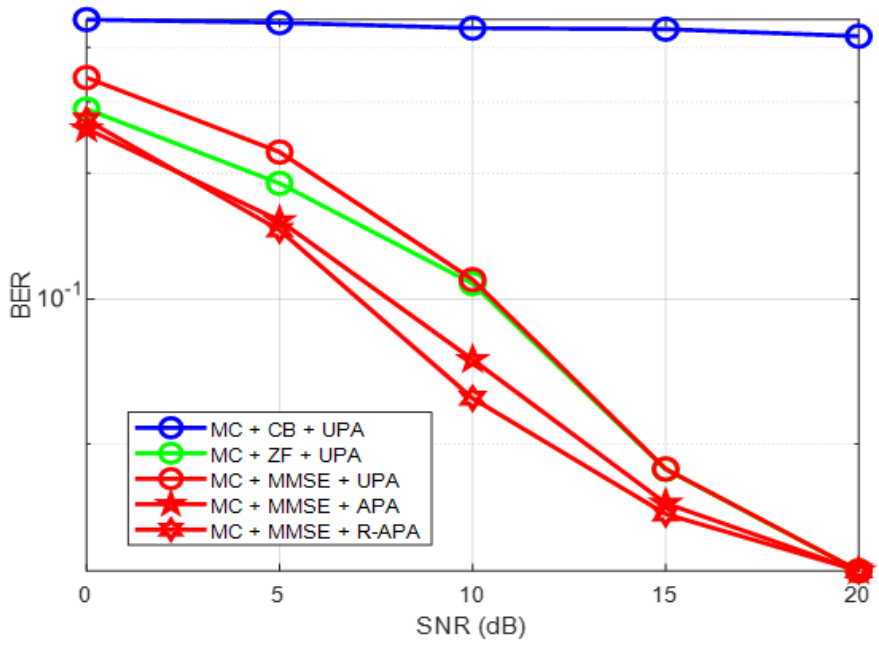

Figure 3.7: System Performance: Multi-Cell with C=4, K = 4 and M = 16.

Finally, we compared both systems with the best precoding and power allocation performances. Note that MC outperforms CF for small values of SNR, however, when the curves get close to 15 dB, CF MMSE + R-APA achieved better performance.

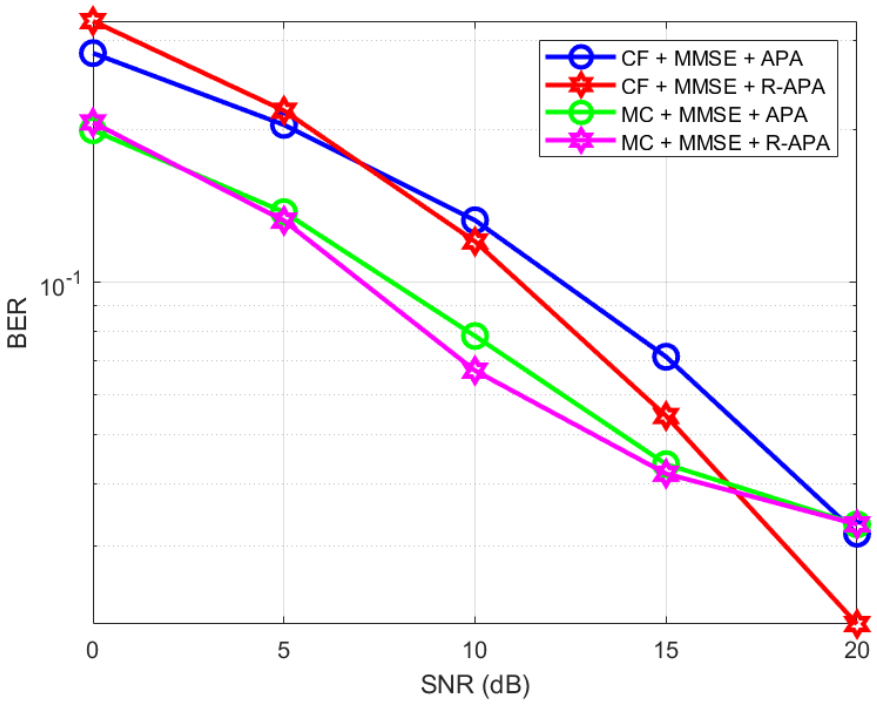

Figure 3.8: Systems Performance: Multi-Cell with C=4, K=4 and M=16 vs Cell-Free with K=16 and M=64.

In this chapter, we have studied linear MMSE precoder calculation and power allocation techniques (UPA, APA and R-APA) derivation. We also presented the computational complexity for each method in this work. Numerical results discussed the development and performance in terms of BER $\times$ SNR and sum-rate characteristics for different setups, assuming the formula: system architecture + precoder + power allocation.

4
Conclusion and Future Work

In this work we have investigated some massive MIMO concepts and applications, along with a vast study of their benefits. The literature review on the subject involved modulation procedure, signal propagation, channel information, channel capacity, uplink description, downlink representation, channel estimation and TDD protocol explanation. Chapter 2 introduces the comparison for the two MIMO architectural setups:

- Multi-Cell: low backhaul requirements and all users are served by only one centralized antenna for a specific area.
- Cell-Free: high backhaul requirements and all users are served by all the distributed antennas simultaneously in the coverage area.

We have also structured each system architecture for the data transmission and reception with different system models. Even though mathematical system model implies different channel coefficients values (due to different number of antennas serving the user in each system), we assume that channel matrices $\mathbf{H}_{cf}^{T} = \mathbf{H}_{mc} = \mathbf{H}$ for mathematical simplification in derivations.

In chapter 3, we considered downlink transmission, presenting three different linear precoding techniques (CB, ZF and MMSE) and three different power allocation methods (UPA, APA and R-APA). For the innovative power allocation R-APA proposed in this work, we calculated a mathematical expression using the MSE cost function, including CSIT imperfections. This expression was then used in an recursive algorithm to recalculates the power allocation matrix. Along with mathematical derivations cited, we perform some simulations and analyses in CF and MC systems scenarios.

Numerical results have illustrated the performance of both systems in terms of BER $\times$ SNR with linear precoders and power allocation algorithms studied. In CF system, MMSE precoder is largely superior when compared to ZF and CB, using the same power allocation technique (UPA). Applying the same framework in MC, the performances of MMSE and ZF precoder designs were similar, however both outperformed CB. APA and R-APA techniques were employed with the linear MMSE precoder in the systems, achieving even better results. The robust approach clearly emphasizes how imperfect CSIT

leads to a decrease in the BER vs. SNR, overcoming all the other power allocation techniques. Comparing both systems best scheme (CF + MMSE + R-APA and MC + MMSE + R-APA), MC has a slight advantage.

The capacity of the systems under study have been evaluated in terms of Sum-Rate × SNR. In CF and MC, MMSE + UPA is equivalent to ZF + UPA, however outperformed CB + UPA considerably. We have noticed the improvement in the overall capacity with the implication of adaptive power allocation techniques. CF sum-rates curves are much higher than those of MC after 10 dB. We have also observed that the number of transmit antennas in each system, alters drastically the capacity.

The computational complexity has also been analyzed in detail for the proposed power allocation method using typical comparisons in the literature. We have demonstrated that R-APA has a small complexity when compared to other techniques.

Finally, MIMO MC systems used in nowadays wireless communication networks (4G and 5G) have proven their efficiency, achieving high rates and reasonable system capacity. MIMO CF systems have shown substantial potential for future wireless technologies, achieving comparable rates to MC systems and excellent system capacity levels. As future works, we can suggest the study of CF high mobility systems, since current systems are considered for scenarios where the mobility of the users are less than 10km/h, due to the application of the TDD protocol and the coherence time interval [40]. Another field of work is CF feasibility and scalability. CF has high computational complexity and fronthaul requirements, when applied to large coverage area with many users, because data are centralized and processed at the CPU.

Bibliography

[1] RAPPAPORT, T. S.; XING, Y.; MACCARTNEY, G. R.; MOLISCH, A. F.; MELLIOS, E. ; ZHANG, J.. **Overview of millimeter wave communications for fifth-generation (5g) wireless networks—with a focus on propagation models**. IEEE Transactions on Antennas and Propagation, 65(12):6213–6230, 2017.

[2] ANDREWS, J. G.; BUZZI, S.; CHOI, W.; HANLY, S. V.; LOZANO, A.; SOONG, A. C. K. ; ZHANG, J. C.. **What will 5g be?** IEEE Journal on Selected Areas in Communications, 32(6):1065–1082, 2014.

[3] LI, P.; DE LAMARE, R. C.. **Distributed iterative detection with reduced message passing for networked MIMO cellular systems**. IEEE Transactions on Vehicular Technology, 63(6):2947–2954, jul 2014.

[4] BIGLIERI, E. R. C.; CONSTANTINIDES, A.; GOLDSMITH, A.; PAULRAJ, A. ; POOR, H. V.. **MIMO Wireless Communication**. Cambridge University Press, 2007.

[5] LU, L.; LI, G. Y.; SWINDLEHURST, A. L.; ASHIKHMIN, A. ; ZHANG, R.. **An overview of massive mimo: Benefits and challenges**. IEEE Journal of Selected Topics in Signal Processing, 8(5):742–758, 2014.

[6] DE LAMARE, R. C.. **Massive mimo systems: Signal processing challenges and future trends**. URSI Radio Science Bulletin, 2013(347):8–20, 2013.

[7] ZHANG, W.; REN, H.; PAN, C.; CHEN, M.; DE LAMARE, R. C.; DU, B. ; DAI, J.. **Large-scale antenna systems with ul/dl hardware mismatch: Achievable rates analysis and calibration**. IEEE Transactions on Communications, 63(4):1216–1229, 2015.

[8] **Towards 6G wireless communication networks: Vision, enabling technologies, and new paradigm shifts**. SCIENCE CHINA Information Sciences, 020300(2016):1–76, 2020.

[9] STUBER, G. L.. **Principles of Mobile Communication**. Kluwerk Academic Publishers, 2002.

[10] FENG, W.; WANG, Y.; GE, N.; LU, J. ; ZHANG, J.. **Virtual mimo in multi-cell distributed antenna systems: Coordinated transmissions with large-scale csit**. IEEE Journal on Selected Areas in Communications, 31(10):2067–2081, 2013.

[11] ZHANG, J.; BJÖRNSON, E.; MATTHAIOU, M.; NG, D. W. K.; YANG, H. ; LOVE, D. J.. **Prospective multiple antenna technologies for beyond 5g**. IEEE Journal on Selected Areas in Communications, 38(8):1637–1660, 2020.

[12] HEATH, R.; PETERS, S.; WANG, Y. ; ZHANG, J.. **A current perspective on distributed antenna systems for the downlink of cellular systems**. IEEE Communications Magazine, 51(4):161–167, 2013.

[13] NGO, H. Q.; ASHIKHMIN, A.; YANG, H.; LARSSON, E. G. ; MARZETTA, T. L.. **Cell-free massive MIMO versus small cells**. IEEE Transactions on Wireless Communications, 16(3):1834–1850, mar 2017.

[14] KARAKAYALI, M.; FOSCHINI, G. ; VALENZUELA, R.. **Network coordination for spectrally efficient communications in cellular systems**. IEEE Wireless Communications, 13(4):56–61, 2006.

[15] NAYEBI, E.; ASHIKHMIN, A.; MARZETTA, T. L.; YANG, H. ; RAO, B. D.. **Precoding and power optimization in cell-free massive MIMO systems**. IEEE Transactions on Wireless Communications, 16(7):4445–4459, jul 2017.

[16] PALHARES, V. M. T.; FLORES, A. R. ; DE LAMARE, R. C.. **Robust mmse precoding and power allocation for cell-free massive mimo systems**. IEEE Transactions on Vehicular Technology, 70(5):5115–5120, 2021.

[17] NAYEBI, E.; ASHIKHMIN, A.; MARZETTA, T. L. ; RAO, B. D.. **Performance of cell-free massive MIMO systems with MMSE and LSFD receivers**. In: 2016 50TH ASILOMAR CONFERENCE ON SIGNALS, SYSTEMS AND COMPUTERS. IEEE, nov 2016.

[18] PALHARES, V. M. T.. **Precoding and resource allocation for cell-free massive mimo systems**, 2020.

[19] FLORES, A. R.; DE LAMARE, R. C.. **Robust Adaptive Power Allocation for the Downlink of Multiple-Antenna Systems**. IEEE Workshop on Statistical Signal Processing Proceedings, p. 206–210, 2021.

[20] FLORES, A. R.; DE LAMARE, R. C.. **Robust and adaptive power allocation techniques for rate splitting based mu-mimo systems**. IEEE Transactions on Communications, p. 1–1, 2022.

[21] MARZETTA, T. L.. **Noncooperative cellular wireless with unlimited numbers of base station antennas**. IEEE Transactions on Wireless Communications, 9(11):3590–3600, 2010.

[22] GOLDSMITH, A.. **Wireless Communications**. Cambridge University Press, 2005.

[23] HOYDIS, J.; KOBAYASHI, M. ; DEBBAH, M.. **Green small-cell networks**. IEEE Vehicular Technology Magazine, 6(1):37–43, 2011.

[24] GESBERT, D.; HANLY, S.; HUANG, H.; SHITZ, S. S.; SIMEONE, O. ; YU, W.. **Multi-cell MIMO cooperative networks: A new look at interference**. IEEE Journal on Selected Areas in Communications, 28(9):1380–1408, dec 2010.

[25] MARSCH, P.; FETTWEIS, G.. **Uplink CoMP under a constrained backhaul and imperfect channel knowledge**. IEEE Transactions on Wireless Communications, 10(6):1730–1742, jun 2011.

[26] DAI, H.; MOLISCH, A. ; POOR, H.. **Downlink capacity of interference-limited MIMO systems with joint detection**. IEEE Transactions on Wireless Communications, 3(2):442–453, mar 2004.

[27] YANG, H.; MARZETTA, T. L.. **Energy efficiency of massive MIMO: Cell-free vs. cellular**. In: 2018 IEEE 87TH VEHICULAR TECHNOLOGY CONFERENCE (VTC SPRING). IEEE, jun 2018.

[28] NGO, H. Q.; TRAN, L.-N.; DUONG, T. Q.; MATTHAIOU, M. ; LARSSON, E. G.. **On the total energy efficiency of cell-free massive mimo**. IEEE Transactions on Green Communications and Networking, 2(1):25–39, 2018.

[29] IRMER, R.; DROSTE, H.; MARSCH, P.; GRIEGER, M.; FETTWEIS, G.; BRUECK, S.; MAYER, H.-P.; THIELE, L. ; JUNGNICKEL, V.. **Coordinated multipoint: Concepts, performance, and field trial results**. IEEE Communications Magazine, 49(2):102–111, feb 2011.

[30] WALRAND, J.; VARAIYA, P.. **High-Performance Communication Networks (Second Edition)**. Elsevier Inc., 2000.

[31] MEDEIROS, J. C. O.. **Princípios de telecomunicações: teoria e prática**. Editora Érica, 2004.

[32] JUNGNICKEL, V.; MANOLAKIS, K.; ZIRWAS, W.; PANZNER, B.; BRAUN, V.; LOSSOW, M.; STERNAD, M.; APELFRÖJD, R. ; SVENSSON, T.. **The role of small cells, coordinated multipoint, and massive mimo in 5g**. IEEE communications magazine, 52(5):44–51, 2014.

[33] E LUIZ A. R. DA SILVA MELLO, M. E. C. R.. **Introdução aos sistemas móveis celulares**, 2002.

[34] TANG, A.; SUN, J. ; GONG, K.. **Mobile propagation loss with a low base station antenna for NLOS street microcells in urban area**. In: IEEE VTS 53RD VEHICULAR TECHNOLOGY CONFERENCE, SPRING 2001. PROCEEDINGS (CAT. NO.01CH37202). IEEE, may 2001.

[35] AKRITAS, A. G.; AKRITAS, E. K. ; MALASCHONOK, G. I.. **Various proofs of sylvester's (determinant) identity**. Mathematics and Computers in Simulation, 42(4):585–593, 1996.

[36] TSE, D.; VISWANATH, P.. **Fundamentals of Wireless Communication**. Cambridge University Press, may 2005.

[37] YACOUB, M. D.. **Foundations of Mobile Radio Engineering**. CRC Press, 1993.

[38] GARG, V. K.; WILKES, J. E.. **Wireless Personal Communication Systems**. Prentice Hall, 1996.

[39] FARUQUE, S.. **Cellular Mobile Radio Engineering**. Artech House, 1996.

[40] ZHANG, J.; CHEN, S.; LIN, Y.; ZHENG, J.; AI, B. ; HANZO, L.. **Cell-free massive mimo: A new next-generation paradigm**. IEEE Access, 7:99878–99888, 2019.

[41] JOHAM, M.; UTSCHICK, W. ; NOSSEK, J.. **Linear transmit processing in mimo communications systems**. IEEE Transactions on Signal Processing, 53(8):2700–2712, 2005.

[42] HAYES, M. H.. **Statistical Digital Signal Processing and Modeling**. John Wiley & Sons, Ltd, apr 1996.

[43] HAYKIN, S.. **Adaptive Filter Theory**. Pearson, jun 2013.

[44] WATKINS, D. S.. **Fundamentals of Matrix Computations**. Wiley, 2014.

[45] SCHARF, L. L.. **Statistical Signal Processing: Detection, Estimation, and Time Series Analysis**. Pearson, jul 1991.

A
Computational Complexity

Note: Consider $\hat{\mathbf{G}}^* = \mathbf{H}$ and $\hat{\mathbf{G}}^T = \mathbf{H}^H$.

A.1
Precoders

A.1.1
MMSE Precoder

$$\mathbf{P}_{\text{MMSE}} = \frac{f_{\text{MMSE}}}{\sqrt{\rho_f}} \left(\hat{\mathbf{G}}^* \hat{\mathbf{G}}^T + \frac{\text{tr}\left(\mathbf{C_w}\right)}{E_{tr}} \mathbf{I} \right)^{-1} \hat{\mathbf{G}}^* \mathbf{N}^{-1} \tag{A-1}$$

with

$$f_{\text{MMSE}} = \sqrt{\frac{E_{tr}}{\text{tr}\left(\tilde{\mathbf{P}} \mathbf{C_s} \tilde{\mathbf{P}}^H\right)}}. \tag{A-2}$$

$\tilde{\mathbf{P}}\mathbf{C_s} \rightarrow MK^2$ multiplications $+ MK\left(K-1\right)$ additions.

$\tilde{\mathbf{P}}\mathbf{C_s}\tilde{\mathbf{P}}^H \rightarrow M^2K$ multiplications $+ M^2\left(K-1\right)$ additions.

$\dfrac{E_{tr}}{\text{tr}\left(\tilde{\mathbf{P}} \mathbf{C_s} \tilde{\mathbf{P}}^H\right)} \rightarrow 1$ division $+ \left(M-1\right)$ additions.

$\sqrt{\dfrac{E_{tr}}{\text{tr}\left(\tilde{\mathbf{P}} \mathbf{C_s} \tilde{\mathbf{P}}^H\right)}} \rightarrow 1$ square root

$\hat{\mathbf{G}}^* \hat{\mathbf{G}}^T \rightarrow M^2K$ multiplications $+ M^2\left(K-1\right)$ additions.

$\dfrac{\text{tr}\left(\mathbf{C_w}\right)}{E_{tr}} \mathbf{I} \rightarrow 1$ division $+ M^2$ multiplications $+ \left(K-1\right)$ additions.

$\hat{\mathbf{G}}^* \hat{\mathbf{G}}^T + \dfrac{\text{tr}\left(\mathbf{C_w}\right)}{E_{tr}} \mathbf{I} \rightarrow M^2$ additions.

$\left(\hat{\mathbf{G}}^* \hat{\mathbf{G}}^T + \dfrac{\text{tr}\left(\mathbf{C_w}\right)}{E_{tr}} \mathbf{I} \right)^{-1} \rightarrow \dfrac{M^2+M}{2}$ divisions

$+ \dfrac{2M^3+3M^2-5M}{6}$ multiplications $+ \dfrac{2M^3+3M^2-5M}{6}$ additions.

$\left(\hat{\mathbf{G}}^* \hat{\mathbf{G}}^T + \dfrac{\text{tr}\left(\mathbf{C_w}\right)}{E_{tr}} \mathbf{I} \right)^{-1} \hat{\mathbf{G}}^* \rightarrow M^2K$ multiplications

$+ MK\left(M-1\right)$ additions.

$$\mathbf{N}^{-1} \rightarrow \frac{K^2+K}{2} \text{ divisions } + \frac{2K^3+3K^2-5K}{6} \text{ multiplications}$$
$$+ \frac{2K^3+3K^2-5K}{6} \text{ additions.}$$
$$\left(\hat{\mathbf{G}}^*\hat{\mathbf{G}}^T + \frac{\text{tr}\left(\mathbf{C_w}\right)}{E_{tr}}\mathbf{I}\right)^{-1}\hat{\mathbf{G}}^*\mathbf{N}^{-1} \rightarrow MK^2 \text{ multiplications}$$
$$+ MK\left(K-1\right) \text{ additions.}$$
$$\frac{f_{\text{MMSE}}}{\sqrt{\rho_f}}\left(\hat{\mathbf{G}}^*\hat{\mathbf{G}}^T + \frac{\text{tr}\left(\mathbf{C_w}\right)}{E_{tr}}\mathbf{I}\right)^{-1}\hat{\mathbf{G}}^*\mathbf{N}^{-1} \rightarrow 1 \text{ division } + MK \text{ multiplications}$$
$$+ 1 \text{ square root}$$

Overall Complexity:

$$\text{Divisions } = \frac{M^2+M}{2} + \frac{K^2+K}{2} + 3$$
$$\text{Multiplications } = 2MK^2 + 3M^2K + M^2 + \frac{2M^3+3M^2-5M}{6}$$
$$+ \frac{2K^3+3K^2-5K}{6} + MK$$
$$= \frac{M^3}{3} + M^2\left(3K+\frac{3}{2}\right) + M\left(2K^2-\frac{5}{6}+K\right) + \frac{2K^3+3K^2-5K}{6}$$
$$\text{Additions } = 2MK\left(K-1\right) + 2M^2\left(K-1\right) + \left(M-1\right) + \left(K-1\right) + M^2$$
$$+ \frac{2M^3+3M^2-5M}{6} + MK\left(M-1\right) + \frac{2K^3+3K^2-5K}{6}$$
$$= \frac{M^3}{3} + M^2\left(3K-1/2\right) + M\left(2K^2-3K+\frac{1}{6}\right) + \frac{2K^3+3K^2+K}{6} - 2$$
$$\text{Square Roots } = 2$$

According to the Big O notation, the complexity of the MMSE precoder is $\mathcal{O}\left(M^3\right)$.

A.1.2 ZF Precoder

$$\mathbf{P}_{\text{ZF}} = \left(\hat{\mathbf{G}}^*\hat{\mathbf{G}}^T\right)^{-1}\hat{\mathbf{G}}^* \tag{A-3}$$

$$\hat{\mathbf{G}}^*\hat{\mathbf{G}}^T \rightarrow M^2K \text{ multiplications } + M^2\left(K-1\right) \text{ additions.}$$
$$\left(\hat{\mathbf{G}}^*\hat{\mathbf{G}}^T\right)^{-1} \rightarrow \frac{M^2+M}{2} \text{ divisions } + \frac{2M^3+3M^2-5M}{6} \text{ multiplications}$$
$$+ \frac{2M^3+3M^2-5M}{6} \text{ additions.}$$
$$\left(\hat{\mathbf{G}}^*\hat{\mathbf{G}}^T\right)^{-1}\hat{\mathbf{G}}^* \rightarrow M^2K \text{ multiplications } + MK\left(M-1\right) \text{ additions.}$$

Overall Complexity:

$$\begin{aligned}
\text{Divisions } &= \frac{M^2+M}{2} \\
\text{Multiplications } &= 2M^2K + \frac{2M^3+3M^2-5M}{6} \\
&= \frac{M^3}{3} + M^2\left(2K+\frac{1}{2}\right) - \frac{5M}{6} \\
\text{Additions } &= M^2(K-1) + \frac{2M^3+3M^2-5M}{6} + MK(M-1) \\
&= \frac{M^3}{3} + M^2\left(2K-\frac{1}{2}\right) - M\left(\frac{5}{6}+K\right)
\end{aligned}$$

According to the Big O notation, the complexity of the ZF precoder is $\mathcal{O}(M^3)$.

If the matrix inversion lemma, [45], is applied to the MMSE, RMMSE and ZF precoders, the complexity can decrease from $\mathcal{O}(M^3)$ to $\mathcal{O}(K^3)$.

A.1.3 CB Precoder

There is no complexity involved in calculating the CB precoder since it is just

$$\mathbf{P}_{\text{CB}} = \hat{\mathbf{G}}^* \tag{A-4}$$

A.2 Precoders + Power Allocation

A.2.1 MMSE Precoder + Power Allocation

$$\begin{aligned}
\mathbf{P}_{\text{MMSE}}\mathbf{N}_{\text{MMSE}} \rightarrow\ & MK^2 \text{ multiplications } + MK(K-1) \text{ additions} \\
& + K \text{ square roots.}
\end{aligned} \tag{A-5}$$

A.2.2 ZF Precoder + Power Allocation

$$\begin{aligned}
\mathbf{P}_{\text{ZF}}\mathbf{N}_{\text{ZF}} \rightarrow\ & MK^2 \text{ multiplications } + MK(K-1) \text{ additions} \\
& + K \text{ square roots.}
\end{aligned} \tag{A-6}$$

A.2.3
CB Precoder + Power Allocation

$$\mathbf{P}_{\mathrm{CB}} \odot \mathbf{N}_{\mathrm{CB}} = \hat{\mathbf{G}}^{*} \odot \mathbf{N}_{\mathrm{CB}} \rightarrow MK \text{ multiplications } + MK \text{ square roots.} \quad \text{(A-7)}$$

A.3
SINR Computation

MMSE Precoder

$$\mathrm{SINR}_{k,\mathrm{MMSE}} = \frac{\rho_f \eta_k \psi_k}{\sigma_w^2 + \rho_f \sum_{i=1, i\neq k}^{K} \eta_i \phi_{k,i} + \rho_f \sum_{i=1}^{K} \eta_i \gamma_{k,i}}, \quad \text{(A-8)}$$

$$\begin{aligned}
&\psi_k = \mathbb{E}\left[\mathbf{p}_k^H \hat{\mathbf{g}}_k^* \hat{\mathbf{g}}_k^T \mathbf{p}_k\right] \\
&\hat{\mathbf{g}}_k^* \hat{\mathbf{g}}_k^T \rightarrow M^2 \text{ multiplications.} \\
&\mathbf{p}_k^H \hat{\mathbf{g}}_k^* \hat{\mathbf{g}}_k^T \rightarrow M^2 \text{ multiplications } + M(M-1) \text{ additions.} \\
&\mathbf{p}_k^H \hat{\mathbf{g}}_k^* \hat{\mathbf{g}}_k^T \mathbf{p}_k \rightarrow M \text{ multiplications } + (M-1) \text{ additions.} \\
&\text{Multiplications } = 2M^2 + M. \\
&\text{Additions } = (M-1)(M+1) \\
&\quad = M^2 - 1.
\end{aligned} \quad \text{(A-9)}$$

$$\begin{aligned}
&\phi_{k,i} = \mathbb{E}\left[\mathbf{p}_i^H \hat{\mathbf{g}}_k^* \hat{\mathbf{g}}_k^T \mathbf{p}_i\right], i \neq k, i = 1, \ldots, K. \\
&\hat{\mathbf{g}}_k^* \hat{\mathbf{g}}_k^T \rightarrow M^2 \text{ multiplications.} \\
&\mathbf{p}_i^H \hat{\mathbf{g}}_k^* \hat{\mathbf{g}}_k^T \rightarrow M^2(K-1) \text{ multiplications } + M(M-1)(K-1) \text{ additions.} \\
&\mathbf{p}_i^H \hat{\mathbf{g}}_k^* \hat{\mathbf{g}}_k^T \mathbf{p}_i \rightarrow M(K-1) \text{ multiplications } + (M-1)(K-1) \text{ additions.} \\
&\text{Multiplications } = M^2 + M^2(K-1) + M(K-1) \\
&\quad = M^2 K + M(K-1) \\
&\text{Additions } = M(M-1)(K-1) + (M-1)(K-1) \\
&\quad = M^2(K-1) - K + 1
\end{aligned} \quad \text{(A-10)}$$

$$
\begin{aligned}
&\boldsymbol{\gamma}_k = \operatorname{diag}\left\{\mathbb{E}\left[\mathbf{P}_{\mathrm{MMSE}}^H \mathbb{E}\left[\tilde{\mathbf{g}}_k^* \tilde{\mathbf{g}}_k^T\right] \mathbf{P}_{\mathrm{MMSE}}\right]\right\} \\
&\hat{\mathbf{g}}_k^* \hat{\mathbf{g}}_k^T \rightarrow M^2 \text{ multiplications.} \\
&\mathbf{P}_{\mathrm{MMSE}}^H \mathbb{E}\left[\tilde{\mathbf{g}}_k^* \tilde{\mathbf{g}}_k^T\right] \rightarrow M^2 K \text{ multiplications } + MK\left(M-1\right) \text{ additions.} \\
&\mathbf{P}_{\mathrm{MMSE}}^H \mathbb{E}\left[\tilde{\mathbf{g}}_k^* \tilde{\mathbf{g}}_k^T\right] \mathbf{P}_{\mathrm{MMSE}} \rightarrow MK^2 \text{ multiplications } + K^2\left(M-1\right) \text{ additions.} \\
&\text{Multiplications } = M^2 + M^2 K + MK^2 \\
&\quad = M^2\left(K+1\right) + MK^2 \\
&\text{Additions } = MK\left(M-1\right) + K^2\left(M-1\right) \\
&\quad = M^2 K + M\left(K^2 - K\right) - K^2
\end{aligned}
\tag{A-11}
$$

$$
\begin{aligned}
&\mathrm{SINR}_{k,\mathrm{MMSE}} = \frac{\rho_f \eta_k \psi_k}{\sigma_w^2 + \rho_f \sum_{i=1, i\neq k}^{K} \eta_i \phi_{k,i} + \rho_f \sum_{i=1}^{K} \eta_i \gamma_{k,i}} \\
&\rho_f \eta_k \psi_k \rightarrow 2 \text{ multiplications.} \\
&\rho_f \sum_{i=1, i\neq k}^{K} \eta_i \phi_{k,i} \rightarrow K \text{ multiplications } + K - 2 \text{ additions.} \\
&\rho_f \sum_{i=1}^{K} \eta_i \gamma_{k,i} \rightarrow K+1 \text{ multiplications } + K - 1 \text{ additions.} \\
&\sigma_w^2 + \rho_f \sum_{i=1, i\neq k}^{K} \eta_i \phi_{k,i} + \rho_f \sum_{i=1}^{K} \eta_i \gamma_{k,i} \rightarrow 2 \text{ additions.} \\
&\text{Divisions } = 1 \\
&\text{Multiplications } = 2K + 3 \\
&\text{Additions } = 2K - 1
\end{aligned}
\tag{A-12}
$$

Overall Complexity:

$$
\begin{aligned}
&\text{Divisions } = 1 \\
&\text{Multiplications } = 2M^2 + M + M^2 K + M\left(K-1\right) + M^2\left(K+1\right) \\
&\quad + MK^2 + 2K + 3 \\
&\quad = M^2\left(2K+3\right) + M\left(K^2 + K\right) + 2K + 3 \\
&\text{Additions } = M^2 - 1 + M^2\left(K-1\right) - K + 1 + M^2 K + M\left(K^2 - K\right) - K^2 + 2K - 1 \\
&\quad = M^2\left(2K\right) + M\left(K^2 - K\right) - K^2 + K + 1
\end{aligned}
\tag{A-13}
$$

Given that $\mathrm{SINR}_{k,\mathrm{MMSE}}$, for $k = 1, \ldots, K$, the complexity of the SINR computation for the MMSE precoder is $\mathcal{O}\left(M^2 K^2\right)$.

A.3.1 ZF Precoder

$$\mathrm{SINR}_{k,\mathrm{ZF}} = \frac{\rho_f \eta_k}{\sigma_w^2 + \rho_f \sum_{i=1}^{K} \eta_i \gamma_{k,i}}, \tag{A-14}$$

$$\begin{aligned}
&\boldsymbol{\gamma}_k = \mathrm{diag}\left\{\mathbb{E}\left[\mathbf{P}_{\mathrm{ZF}}^H \mathbb{E}\left[\tilde{\mathbf{g}}_k^* \tilde{\mathbf{g}}_k^T\right] \mathbf{P}_{\mathrm{ZF}}\right]\right\} \\
&\mathbb{E}\left[\tilde{\mathbf{g}}_k^* \tilde{\mathbf{g}}_k^T\right] \rightarrow M^2 \text{ multiplications.} \\
&\mathbf{P}_{\mathrm{ZF}}^H \mathbb{E}\left[\tilde{\mathbf{g}}_k^* \tilde{\mathbf{g}}_k^T\right] \rightarrow M^2 K \text{ multiplications } + MK\left(M-1\right) \text{ additions.} \\
&\mathbf{P}_{\mathrm{ZF}}^H \mathbb{E}\left[\tilde{\mathbf{g}}_k^* \tilde{\mathbf{g}}_k^T\right] \mathbf{P}_{\mathrm{ZF}} \rightarrow MK^2 \text{ multiplications } + K^2\left(M-1\right) \text{ additions.} \\
&\text{Multiplications } = M^2 + M^2 K + MK^2 \\
&\quad = M^2\left(K+1\right) + MK^2 \\
&\text{Additions } = MK\left(M-1\right) + K^2\left(M-1\right) \\
&\quad = M^2 K + M\left(K^2 - K\right) - K^2
\end{aligned} \tag{A-15}$$

$$\begin{aligned}
&\mathrm{SINR}_{k,\mathrm{ZF}} = \frac{\rho_f \eta_k}{\sigma_w^2 + \rho_f \sum_{i=1}^{K} \eta_i \gamma_{k,i}} \\
&\rho_f \eta_k \rightarrow 1 \text{ multiplications.} \\
&\rho_f \sum_{i=1}^{K} \eta_i \gamma_{k,i} \rightarrow K+1 \text{ multiplications } + K-1 \text{ additions.} \\
&\sigma_w^2 + \rho_f \sum_{i=1}^{K} \eta_i \gamma_{k,i} \rightarrow 1 \text{ additions.} \\
&\text{Divisions } = 1 \\
&\text{Multiplications } = K+2 \\
&\text{Additions } = K
\end{aligned} \tag{A-16}$$

Overall Complexity:

$$\begin{aligned}
&\text{Divisions } = 1 \\
&\text{Multiplications } = M^2\left(K+1\right) + MK^2 + K + 2 \\
&\text{Additions } = M^2 K + M\left(K^2 - K\right) - K^2 + K
\end{aligned} \tag{A-17}$$

Given that $\mathrm{SINR}_{k,\mathrm{ZF}}$, for $k = 1, \ldots, K$, the complexity of the SINR computation for the ZF precoder is $\mathcal{O}\left(M^2 K^2\right)$.

A.3.2
CB Precoder

$$\mathrm{SINR}_{k,\mathrm{CB}} = \frac{\rho_f \left(\sum_{m=1}^{M} \sqrt{\eta_{mk}}\alpha_{mk}\right)^2}{\sigma_w^2 + \rho_f \sum_{i=1}^{K}\sum_{m=1}^{M} \eta_{mi}\beta_{mk}\alpha_{mi}}, \tag{A-18}$$

$$\begin{aligned}
&\sum_{m=1}^{M} \sqrt{\eta_{mk}}\alpha_{mk} \rightarrow M \text{ multiplications } + (M-1) \text{ additions} + M \text{ square roots.}\\
&\rho_f \left(\sum_{m=1}^{M} \sqrt{\eta_{mk}}\alpha_{mk}\right)^2 \rightarrow 2 \text{ multiplications.}\\
&\sigma_w^2 + \rho_f \sum_{i=1}^{K}\sum_{m=1}^{M} \eta_{mi}\beta_{mk}\alpha_{mi} \rightarrow (2MK+1) \text{ multiplications}\\
&\quad + (M-1)(K-1) + 1 \text{ additions.}
\end{aligned} \tag{A-19}$$

Overall Complexity:

$$\begin{aligned}
&\text{Divisions } = 1\\
&\text{Multiplications } = M + 2 + 2MK + 1\\
&\quad = M(2K+1) + 3\\
&\text{Additions } = M - 1 + (M-1)(K-1) + 1\\
&\quad = MK - K + 1\\
&\text{Square Roots } = M
\end{aligned} \tag{A-20}$$

Given that $\mathrm{SINR}_{k,\mathrm{CB}}$, for $k = 1, \ldots, K$, the complexity of the SINR computation for the CB precoder is $\mathcal{O}(MK^2)$.

A.4
Power Allocation

A.4.1
APA Algorithm

$$\mathbf{N}[i+1] = \mathbf{N}[i] - \mu\left(-f^{-1}\sqrt{\rho_f}\mathbf{P}^H\hat{\mathbf{G}}^*\mathbf{C_s} + f^{-2}\rho_f\mathbf{P}^H\hat{\mathbf{G}}^*\hat{\mathbf{G}}^T\mathbf{P}\mathbf{N}[i]\mathbf{C_s}\right) \tag{A-21}$$

$$
\begin{aligned}
&\mathbf{P}^H\hat{\mathbf{G}}^* \rightarrow MK^2 \text{ multiplications } + K^2\left(M-1\right) \text{ additions.}\\
&\mathbf{P}^H\hat{\mathbf{G}}^*\mathbf{C_s} \rightarrow K^3 \text{ multiplications } + K^2(K-1) \text{ additions.}\\
&f^{-1}\sqrt{\rho_f} \rightarrow 1 \text{ division } + 1 \text{ square root.}\\
&f^{-1}\sqrt{\rho_f}\mathbf{P}^H\hat{\mathbf{G}}^*\mathbf{C_s} \rightarrow K^2 \text{ multiplications.}\\
&\mathbf{P}^H\hat{\mathbf{G}}^*\hat{\mathbf{G}}^T \rightarrow MK^2 \text{ multiplications } + MK\left(K-1\right) \text{ additions.}\\
&\mathbf{P}^H\hat{\mathbf{G}}^*\hat{\mathbf{G}}^T\mathbf{P} \rightarrow MK^2 \text{ multiplications } + K^2(M-1) \text{ additions.}\\
&\mathbf{P}^H\hat{\mathbf{G}}^*\hat{\mathbf{G}}^T\mathbf{P}\mathbf{N}[i] \rightarrow K^3 \text{ multiplication } + K^2\left(K-1\right) \text{ additions.}\\
&\mathbf{P}^H\hat{\mathbf{G}}^*\hat{\mathbf{G}}^T\mathbf{P}\mathbf{N}[i]\mathbf{C_s} \rightarrow K^3 \text{ multiplications } + K^2\left(K-1\right) \text{ additions.}\\
&f^{-2}\rho_f \rightarrow 1 \text{ division } + 1 \text{ multiplication.}\\
&f^{-2}\rho_f\mathbf{P}^H\hat{\mathbf{G}}^*\hat{\mathbf{G}}^T\mathbf{P}\mathbf{N}[i]\mathbf{C_s} \rightarrow K^2 \text{ multiplications.}\\
&-f^{-1}\sqrt{\rho_f}\mathbf{P}^H\hat{\mathbf{G}}^*\mathbf{C_s} + f^{-2}\rho_f\mathbf{P}^H\hat{\mathbf{G}}^*\hat{\mathbf{G}}^T\mathbf{P}\mathbf{N}[i]\mathbf{C_s} \rightarrow K^2 \text{ additions.}\\
&\mathbf{N}[i] - \mu\left(-f^{-1}\sqrt{\rho_f}\mathbf{P}^H\hat{\mathbf{G}}^*\mathbf{C_s} + f^{-2}\rho_f\mathbf{P}^H\hat{\mathbf{G}}^*\hat{\mathbf{G}}^T\mathbf{P}\mathbf{N}[i]\mathbf{C_s}\right)\\
&\quad \rightarrow K^2 \text{ multiplications } + K^2 \text{ additions.}
\end{aligned}
\tag{A-22}
$$

Overall Complexity:

$$
\begin{aligned}
&\text{Divisions } = 2\\
&\text{Multiplications } = T_{\text{APA}}\left(MK^2 + K^3 + K^2 + MK^2 + MK^2 + K^3 + K^3 + 1 + K^2 + K^2\right)\\
&\quad = T_{\text{APA}}\left(3MK^2 + 3K^3 + 3K^2 + 1\right)\\
&\text{Additions } = T_{\text{APA}}\left(K^2\left(M-1\right) + K^2\left(K-1\right) + MK\left(K-1\right) + K^2\left(M-1\right)\right.\\
&\quad \left. + K^2\left(K-1\right) + K^2\left(K-1\right) + K^2 + K^2\right)\\
&\quad = T_{\text{APA}}\left(M\left(3K^2 - K\right) + 3K^3 - 3K^2\right)\\
&\text{Square Roots } = T_{\text{APA}}\left(1\right)
\end{aligned}
\tag{A-23}
$$

According to the Big O notation, the complexity of the APA algorithm is $\mathcal{O}\left(T_{\text{APA}}MK^2\right)$.

A.4.2 UPA Algorithm

$$
\begin{aligned}
\eta_k &= 1/\left(\max_m \sum_{i=1}^{K} \delta_{mi}\right),\ k = 1, \ldots, K,\\
\boldsymbol{\delta}_m &= \text{diag}\left\{\mathbb{E}\left[\mathbf{p}_m^T\mathbf{p}_m^*\right]\right\},\ \text{for } m = 1, \ldots, M.
\end{aligned}
\tag{A-24}
$$

$$\begin{aligned}
\text{diag}\left\{\mathbb{E}\left[\mathbf{p}_m^T \mathbf{p}_m^*\right]\right\} &\rightarrow MK^2 \text{ multiplications.} \\
\sum_{i=1}^{K} \delta_{mi} &\rightarrow M\left(K-1\right) \text{ additions.} \\
\max_m \sum_{i=1}^{K} \delta_{mi} &\rightarrow M \\
1/\left(\max_m \sum_{i=1}^{K} \delta_{mi}\right) &\rightarrow 1 \text{ division.}
\end{aligned} \tag{A-25}$$

Overall Complexity:

$$\begin{aligned}
&\text{Divisions} = 1 \\
&\text{Multiplications} = MK^2 \\
&\text{Additions} = M\left(K-1\right) \\
&\text{Sorting} = M
\end{aligned} \tag{A-26}$$

According to the Big O notation, the complexity of the UPA algorithm is $\mathcal{O}\left(MK^2\right)$.